DEVELOPMENT OF OPTIMAL CONTROL MODES FOR ADVANCED TECHNOLOGY PROPULSION SYSTEMS

Gerald J. Michael, et al

United Aircraft Research Laboratories

Prepared for:

Office of Naval Research

March 1974

UNCLASSIFIED

SECURITY CLASSIFICATION OF THIS PAGE (When Data Entered)

REPORT DOCUMENTATION PAGE

READ INSTRUCTIONS BEFORE COMPLETING FORM

1 REPORT NUMBER: N911620-2	2. GOVT ACCESSION NO.
3. RECIPIENT'S CATALOG NUMBER: AD 775337	
4 TITLE (and Subtitle): DEVELOPMENT OF OPTIMAL CONTROL MODES FOR ADVANCED TECHNOLOGY PROPULSION SYSTEMS	5 TYPE OF REPORT & PERIOD COVERED: Annual Technical Report 1 Feb. 1973 - 31 Jan. 1974
	6 PERFORMING ORG. REPORT NUMBER
7 AUTHOR(s): Gerald J. Michael, Florence A. Farrar	8. CONTRACT OR GRANT NUMBER(s): N00014-73-C-0281
9 PERFORMING ORGANIZATION NAME AND ADDRESS: United Aircraft Research Laboratories, 400 Main Street, East Hartford, Connecticut 06108	10. PROGRAM ELEMENT, PROJECT, TASK AREA & WORK UNIT NUMBERS: NR 215-219
11 CONTROLLING OFFICE NAME AND ADDRESS: Office of Naval Research (Code 411-7), Department of the Navy, Arlington, Virginia 22217	12 REPORT DATE: March 1974
	13. NUMBER OF PAGES: 57 60
14 MONITORING AGENCY NAME & ADDRESS (If different from Controlling Office)	15 SECURITY CLASS. (of this report): UNCLASSIFIED
	15a. DECLASSIFICATION DOWNGRADING SCHEDULE

16 DISTRIBUTION STATEMENT (of this Report)

Approved for public release; distribution unlimited.

17 DISTRIBUTION STATEMENT (of the abstract entered in Block 20, if different from Report)

18 SUPPLEMENTARY NOTES

Reproduction in whole or in part is permitted for any purpose of the United States Government.

19 KEY WORDS (Continue on reverse side if necessary and identify by block number)

Multivariable Engine Control
Optimal Engine Control
Variable Cycle Turbofan Control
Engine Acceleration Time
Integrated Inlet-Engine Control
Internal Compression Supersonic Inlet

20 ABSTRACT (Continue on reverse side if necessary and identify by block number)

A nonlinear multivariable feedback controller was defined for the idle to military operating regime (9 to 100 percent thrust) of the Pratt & Whitney Aircraft F401 variable cycle turbofan engine. The analytical design involved (1) linearizing the F401 engine dynamics about five steady-state operating points between idle and military thrust, (2) applying linear optimal control synthesis methods at each point, and (3) combining the five optimal linear

(Continued on reverse side)

DD FORM 1 JAN 73 1473 EDITION OF 1 NOV 65 IS OBSOLETE

UNCLASSIFIED

SECURITY CLASSIFICATION OF THIS PAGE (When Data Entered)

20. ABSTRACT (Continued)

controllers into a single nonlinear controller which has feedback gains that are scheduled with high compressor speed. Variable fan, compressor and exhaust geometries as well as main burner fuel flow are coordinated by the controller to achieve rapid engine dynamic response.

Engine accelerations from idle to military thrust levels with the defined nonlinear (optimal) controller were computed using a detailed digital nonlinear simulation of the engine. These accelerations were compared with those obtained using a conventional controller designed to provide rapid thrust response. The optimal controller provided significantly faster F401 engine model acceleration from idle to military thrust, without exceeding temperature or stability margin constraints. Moreover, the optimal controller moved exhaust and fan geometries in a significantly different manner than the conventional controller.

An integrated inlet-engine controller was also defined for the F401 engine and a mathematical model of an internal compression supersonic inlet. The inlet had variable throat and bypass geometries and was interfaced with the F401 engine simulation for a flight condition of 40,000 ft and Mach 2.2. Closed-loop propulsion system response to simulated afterburner ignition was evaluated for separate inlet-engine controls and for the integrated controller.

The integrated controller provided closed-loop regulation which was as good as or better than the separate controls for all critical inlet and engine variables. Also, the improved regulation was accomplished using considerably smaller control positions and rates. The improvement in inlet-engine dynamic performance with the integrated controller was due primarily to cross-feedback from the engine state variables to the inlet control variables.

Annual Technical Report

DEVELOPMENT OF OPTIMAL CONTROL MODES FOR ADVANCED TECHNOLOGY PROPULSION SYSTEMS

Gerald J. Michael

Florence A. Farrar

United Aircraft
Research Laboratories

UNITED AIRCRAFT CORPORATION

EAST HARTFORD, CONNECTICUT 06108

This research was sponsored by the Office of Naval Research
under Contract N00014-73-C-0281.

ib

FOREWORD

This annual technical report documents research performed from 1 February 1973 to 31 January 1974 under Office of Naval Research Contract N00014-73-C-0281. The research program is being conducted at United Aircraft Research Laboratories (UARL), East Hartford, Connecticut 06108. Mr. Govert Flohil is serving as the ONR Scientific Officer.

This report is issued as UARL Report N911620-2.

Report N911620-2

Development of Optimal Control Model
for Advanced Technology Propulsion Systems

TABLE OF CONTENTS

Report R911620-2

Development of Optimal Control Modes for Advanced Technology Propulsion Systems

SUMMARY

A nonlinear multivariable feedback controller was defined for the idle to military operating regime (9 to 100 percent thrust) of the Pratt & Whitney Aircraft F401 variable cycle turbofan engine. The analytical design involved (1) linearizing the F401 engine dynamics about five steady-state operating points between idle and military thrust, (2) applying linear optimal control synthesis methods at each point, and (3) combining the five optimal linear controllers into a single nonlinear controller which has feedback gains that are scheduled with high compressor speed. Variable fan, compressor and exhaust geometries as well as main burner fuel flow are coordinated by the controller to achieve rapid engine dynamic response.

Engine accelerations from idle to military thrust levels with the defined nonlinear (optimal) controller were computed using a detailed digital nonlinear simulation of the engine. These accelerations were compared with those obtained using a conventional controller designed to provide rapid thrust response. The optimal controller provided significantly faster F401 engine model acceleration from idle to military thrust, without exceeding temperature or stability margin constraints. Moreover, the optimal controller moved exhaust and fan geometries in a significantly different manner than the conventional controller.

An integrated inlet-engine controller was also defined for the F401 engine and a mathematical model of an internal compression supersonic inlet. The inlet had variable throat and bypass geometries and was interfaced with the F401 engine simulation for a flight condition of 40,000 ft and Mach 2.2. Closed-loop propulsion system response to simulated afterburner ignition was evaluated for separate inlet-engine controls and for the integrated controller.

The integrated controller provided closed-loop regulation which was as good as or better than the separate controls for all critical inlet and engine variables. Also, the improved regulation was accomplished using considerably smaller control positions and rates. The improvement in inlet-engine dynamic performance with the integrated controller was due primarily to cross-feedback from the engine state variables to the inlet control variables.

RESULTS AND CONCLUSIONS

1. A nonlinear multivariable feedback controller was developed for operation of the F401 variable geometry turbofan engine between idle and military thrust conditions (9 percent and 100 percent thrust, respectively). The piecewise-linear/piecewise-optimal approach to nonlinear control synthesis, developed and reported under a previous ONR contract (Ref. 1), was used to define the controller. Thrust response for nonlinear multivariable control was approximately 30 percent faster than that for the conventional controller, i.e., the 98-percent thrust point was reached in 2.32 sec versus 3.40 sec for conventional control. Both controllers avoided engine overtemperatures and provided similar fan and compressor stability margins.

2. The nonlinear multivariable controller changed fan inlet guide vane positions and jet exhaust area in a manner significantly different from the conventional controller. For the optimal control mode, fan inlet guide vane changes led the steady-state schedule (i.e., the guide vane versus fan speed schedule programmed for steady-state F401 operation), and for conventional control they lagged the steady-state schedule. Jet exhaust area, with the optimal controller, did not move far from its initial position until the fan stability margin had begun to increase. At that time, exhaust area decreased rapidly to its bottom position limit and then increased rapidly to its final steady-state value. In the conventional control mode, exhaust area first increased rapidly, remained constant for a time, and then decreased to its steady-state value.

3. A mathematical model of an internal compression supersonic inlet was interfaced with the F401 engine simulation at a flight condition of 40,000 ft and Mach 2.2, and an integrated inlet-engine controller was designed for that operating point. Integrated control also was synthesized using the piecewise-linear/piecewise-optimal techniques. The integrated controller regulated all critical inlet and engine variables as well as, or better than, the separately designed system. The improved performance was accomplished using considerably smaller control positions and rates, and was due to inlet-engine cross-feedback in the controller.

INTRODUCTION

Advanced technology propulsion systems consist of inlet-engine combinations which incorporate a variety of variable geometry features. Traditional control synthesis procedures appear to be inadequate to exploit the full performance capabilities of advanced technology propulsion systems because the traditional techniques do not properly treat the parameter interaction which exists in these nonlinear multivariable systems. However, modern methods based on a state variable description of system dynamics and the use of optimization procedures to generate feedback control provide the necessary analytical techniques.

The piecewise-linear/piecewise-optimal control synthesis approach, in particular, is attractive because it provides a means to analyze the nonlinear aspects of the propulsion system controller design problem. In addition, there are no compromises in its ability to handle the multivariable properties of the system. This control design concept was developed by UARL in a previous program with ONR (Ref. 1). Optimal multivariable feedback controllers are developed for each point about which the dynamic system to be controlled is linearized. Nonlinear feedback control is then constructed by scheduling the optimal linear controllers with system state. The nonlinear characteristics of the dynamics influence the analysis only in the initial phase during piecewise linearization and in the final phase when the nonlinear controller is implemented and evaluated. In a previous program (Ref. 2), this technique was applied to a detailed nonlinear model of the Pratt & Whitney Aircraft F401 variable cycle turbofan engine and an optimal multivariable feedback controller was defined for high power engine operation (80 to 100 percent thrust). Calculated F401 engine response using this controller was significantly faster than the response for a state-of-the-art conventional control*.

The principal objective of the studies described in this report was to define and evaluate an optimal multivariable controller capable of accelerating the F401 engine model from idle (9 percent thrust) to military (100 percent thrust) conditions. Another major objective was to determine performance advantages and characteristics of an inlet-engine feedback controller designed by treating the inlet and engine as a single integrated dynamic system.

*The conventional control used for comparison in Ref. 2, as well as in this report, is the P&WA fast accel controller.

SYNTHESIS OF AN OPTIMAL FEEDBACK CONTROL SYSTEM

The application to the F401 engine of the piecewise-linear/piecewise-optimal method for synthesizing multivariable feedback control is described in this section. The objective was to synthesize a multivariable controller which would provide significantly faster accelerations than those resulting for a conventional control mode, while satisfying temperature, stability, control position and control actuation rate constraints. Engine input, state and output variables which are appropriate for the synthesis procedure are introduced initially, and the linearization of engine dynamics is described. Linear optimal control methods used to compute feedback gains are outlined next, and the development of the nonlinear feedback controller from the sets of linear gains is discussed. Finally, the particular optimal multivariable controller developed for the F401 engine is detailed, and calculated engine response for the optimal multivariable controller is compared with that which can be obtained for a conventional controller.

Multivariable Engine Dynamics

The first step in applying the piecewise-linear/piecewise-optimal control technique is to define engine control variables, state variables, and output variables. The F401 engine has variable exhaust, fan, and compressor geometries. Accordingly, the control variables chosen for this study were:

- jet exhaust area (u_1)
- fan inlet guide vanes (u_2)
- rear compressor variable vanes (u_3)
- main burner fuel flow (u_4)

The engine state variables chosen were:

- fan turbine inlet temperature (x_1)
- main burner pressure (x_2)
- fan speed (x_3)
- high compressor speed (x_4)
- afterburner pressure (x_5)

These independent variables are sufficient to establish the F401 operating condition and to define the dynamic path of the engine. The engine output variables were selected after consideration of engine steady-state operating requirements. For efficient steady-state performance the positions of the fan inlet guide vanes and the rear compressor variable vanes are scheduled as functions of fan speed, N_1, and high compressor speed, N_2, respectively. It is therefore desirable that, in the steady state, the vane positions be at their scheduled values. This was accomplished by (1) defining the fan inlet guide vanes and the rear compressor variable vanes as the first two output variables, y_1 and y_2, respectively, and (2) commanding that y_1 and y_2 achieve their steady-state scheduled positions as a function of steady-state N_1, N_2, respectively. This procedure allowed transient vane operation to be optimized while insuring proper steady-state positioning. The remaining engine output variables considered were:

- thrust (y_3)
- high turbine inlet temperature (y_4)
- fan corrected airflow (y_5)
- fan stability margin (y_6)
- compressor stability margin (y_7)

Table I lists values of the steady-state engine variables for sea-level static conditions at five power-lever angle (PLA) design points: PLA = 20, 35, 47, 60 and 73 deg. For convenience, all engine parameters except fan and compressor vanes and fan and compressor stability margins have been normalized to 1.0 at PLA = 73 deg. The vane positions are defined as ratios of their maximum positions, and the two stability margins are given as ratios of one (a smaller value indicates reduced stability margin). These data are also shown in Fig. 1, where linear interpolation has been used between design points to define the steady-state values as functions of power-lever angle. The 20-deg PLA is the engine idle condition while the 73-deg PLA represents the military rating condition (maximum nonafterburning thrust).

The next step in the synthesis procedure is to linearize the engine dynamics at a set of points along the steady-state operating line. Linear dynamics at a steady-state operating point can be represented by

$$\begin{aligned} \delta\dot{x} &= A\delta x + B\delta u \\ \delta y &= C\delta x + D\delta u \end{aligned} \tag{1}$$

where the vector δx represents perturbations in the five engine state variables, the vector δy represents perturbations in the seven output variables, and the vector δu represents perturbations in the four control variables. The constant matrices A, B, C and D consist of appropriate partial derivatives of the engine dynamic response evaluated at the given operating point. Linearized engine dynamics at PLA = 20, 35, 47, 60 and 73 deg, calculated in a previous program (Ref. 1), were used here for control synthesis. The calculated values of A and B at each of the five control design points are presented in Table II where the control, state, and output variable ordering is as previously defined. The corresponding C and D matrices are presented in Table III. The matrix elements were determined by applying a system identification technique to input-output-state data generated by a nonlinear dynamic computer simulation of the F401 engine (Ref. 3). Details of the system identification procedure used are contained in Ref. 1.

Four integrators, one for each control input, were also added to the linear engine model of Eq. (1). These integrators are used in the optimal controller to insure zero steady-state errors in commanded engine response. Augmenting the linear engine dynamics with the integrators results in the following equations for the controlled plant:

$$\begin{aligned} \delta\dot{x} &= A\delta x + B\delta u \\ \delta\dot{u} &= \delta w \\ \delta y &= C\delta x + D\delta u \end{aligned} \tag{2}$$

The linear engine model with the integrators is shown in Fig. 2(a).

Calculation of Optimal Feedback Gains

Optimal linear feedback gains were computed at the five selected control design points by minimizing the following performance index:

$$J = \tfrac{1}{2}\int_0^\infty \Big[q_1(IGV)^2 + q_2(RCVV)^2 + q_3(F)^2 + q_4(T_{IT})^2 + q_5(\dot{FSM})^2 + q_6(\dot{CSM})^2 + r_1(\dot{A}_j) + r_2(\dot{IGV}) + r_3(\dot{RCVV})^2 + r_4(\dot{w}_f)^2 \Big] dt \tag{3}$$

where q_i, r_i are weighting factors and

IGV $\triangleq$ perturbed fan inlet guide vanes

RCVV $\triangleq$ perturbed rear compressor variable vanes

$F \triangleq$ perturbed thrust

$T_{IT} \triangleq$ perturbed high turbine inlet temperature

$FSM \triangleq$ perturbed fan stability margin

$CSM \triangleq$ perturbed compressor stability margin

$A_j \triangleq$ perturbed jet exhaust area

$w_f \triangleq$ perturbed main burner fuel flow

The dot notation denotes time rate-of-change of a parameter. The solution to the linear optimal control problem, i.e., the minimization of J (Ref. 4), leads to the standard optimal control structure shown in Fig. 2(b). The constant matrices G_1 and G_2 (Fig. 2(b)) are the optimal closed-loop feedback gain matrices. The gain matrix M has been added to the controller to permit the consideration of command inputs δz.

To insure zero steady-state errors between desired and actual output, an integral control structure (Fig. 2(c)) was derived from the standard form. A method for converting from the common linear optimal structure to an integral control which retains the desired optimal control characteristics was developed in Ref. 1. The integral control gain matrices H and L are determined from the system matrices A, B, C and D and the standard optimal gain matrices G_1 and G_2. Since there are four independent engine control variables, the steady-state values of four engine output variables can be specified independently. The vector v (Fig. 2(c)) represents those four engine output variables whose steady-state values are to be specified.

Nonlinear Feedback Control Synthesis

After the H and L matrices (Fig. 2(c)) were computed at each control design point, linear interpolation was used to define the matrices as functions of high compressor speed, N_2, between design points, i.e., $H = H(N_2)$, $L = L(N_2)$. If H and L are defined in this manner, the optimal control is

$$u^*(t) = \int_{x(0)}^{x(t)} L(N_2)\, dx + \int_0^{t} H(N_2) \left[v(\tau) - z(\tau)\right] d\tau + u^*(0) \qquad (4)$$

The vectors v and z are

v_1 = fan inlet guide vanes	z_1 = commanded v_1
v_2 = rear compressor variable vanes	z_2 = commanded v_2
v_3 = thrust	z_3 = commanded v_3
v_4 = high turbine inlet temperature	z_4 = commanded v_4

The functions z_1, z_2, z_3, z_4 were coordinated such that the engine was commanded from initial to final conditions both of which were always on its steady-state operating line (as defined in Fig. 1) when operating point was changed. The resulting nonlinear closed-loop control structure is shown in Fig. 3. For convenience, the engineering symbols used in Fig. 3 for the engine variables denote actual rather than perturbational values.

Characteristics of the Optimal Multivariable Controller Developed for the F401 Engine

The performance index weightings q_i, r_i (see Eq. (3) for definitions) were selected at each control design point so that the resulting controller feedback gains (1) produced a rapid engine acceleration and (2) avoided exceeding maximum allowable control actuation rates, maximum control positions, and minimum allowable fan and compressor stability margins (stability must be greater than zero). Table IV presents maximum and minimum limits on F401 control positions and rates. Table V lists a set of weightings for which engine response with the optimal controller will be shown. The higher thrust weightings, q_3, at PLA = 47, 60 and 73 deg (Table V) result in a rapid thrust response during that part of the transient where compressor and fan stability margins pose no problem. The large weightings on high turbine inlet temperature, q_4, at PLA = 20 and 35 deg result in a very rapid temperature response, which in turn helps to provide a rapid engine acceleration. The even larger weighting on temperature at PLA = 47 deg regulates the temperature response when temperature is close to its maximum commanded value, and thereby prevents overtemperature.

The weightings on rate-of-change of fan stability margin, q_5, at PLA = 47 and 60 deg (Table V) permit rapid accelerations at high power levels without surging the fan (e.g., engine accelerations from 80 to 100 percent thrust). Such a weighting is not necessary at the idle condition (PLA = 20 deg) because the large weighting there on rate-of-change of jet exhaust area, r_1, protects against fan surge. Also, it was found that if r_1 were chosen too small at PLA = 20 deg, the jet area would respond to a large step in PLA by immediately decreasing to its bottom position limit. Jet area would then remain there during most of the resulting transient

before increasing to its steady-state value. This presented a problem, since the movements of the remaining three controls were being defined on the basis of a jet area which was free to move in either a positive or negative direction. Consequently, the movements of these three controls (fuel flow, fan inlet guide vanes, rear compressor variable vanes) became uncoordinated with the jet area movement, and poor closed-loop performance resulted. The larger weighting on rate-of-change of jet area at PLA = 20 deg thus serves the dual purposes of (1) maintaining coordination between all four control variables by preventing the jet area from operating on its bottom limit for a long period of time, and (2) preventing fan surge by not allowing the jet area to immediately decrease rapidly after a step PLA change.

The high weighting on rate-of-change of compressor stability margin, q_6, at PLA = 20 deg (Table V) insures adequate compressor margin at the beginning of the transient, where compressor stall is most likely to occur. Increased levels of compressor margin are also obtained by not allowing the rear compressor variable vanes to move rapidly away from their steady-state schedule during the initial stages of the transient. This is the purpose of the high weightings at PLA = 20 and 35 deg on rate-of-change of compressor vanes, r_3.

Feedback gain matrices H and L which result for the weightings of Table V are presented in Table VI. Recall that intermediate values of H and L were computed for the optimal controller by interpolating linearly with N_2. Consequently, H and L can be regarded as continuous functions of N_2 between the end points shown in Table VI.

Comparison of F401 Engine Response with Optimal Multivariable and Conventional Controllers

The optimal multivariable feedback controller (Fig. 3) having the parameters described in the previous section was implemented on the UARL nonlinear computer simulation of the F401 engine (Ref. 3). Engine response for an acceleration command from idle to military thrust, i.e., a step change in PLA from 20 deg (9 percent thrust) to 73 deg (100 percent thrust), was calculated. The results are shown in Figs. 4 through 10. Figures 4 through 8 show time responses for the following engine variables, respectively: thrust, high turbine inlet temperature, compressor and fan stability margins, fan and compressor speeds, airflow, exhaust area and fuel flow. Changes in the positions of the fan inlet guide vanes and rear compressor variable vanes are plotted versus fan and compressor speeds in Figs. 9 and 10, respectively. Fan and compressor variable geometries are presented as functions of spool speeds to more clearly depict the relationship between transient and steady-state vane positions. Comparative engine response data for an F401 conventional controller, which was designed to provide rapid engine acceleration, are also shown in Figs. 4 through 10. Conventional response data were generated

by the Florida Research and Development Center of Pratt & Whitney Aircraft using an F401 engine deck similar to that provided for UARL. However, there are slight differences in the decks which cause the small mismatch evident between the two sets of results at the steady-state operating points.

Thrust response for the optimal controller is approximately 30 percent more rapid than for the conventional controller (Fig. 4). That is, the optimal controller thrust response reached the 98-percent point in 2.32 sec, while conventional thrust response reached the same point in 3.40 sec. The high turbine inlet temperature response for the optimal control was also significantly faster than the conventional temperature response (Fig. 5(a)). This difference contributed to the thrust improvement for the optimal system. Minimum levels of compressor and fan stability margins were similar for the two types of control (Figs. 5(b) and 5(c)), as were the fan and compressor speed and the airflow responses (Fig. 6).

Comparing time histories of the four engine control variables for the different controllers following the step PLA command (Figs. 7 through 10) provides insight into how the optimal controller achieved its rapid acceleration. The optimal controller moved jet exhaust area (Fig. 7) and fan inlet guide vanes (Fig. 9) in a manner distinctly different from the corresponding conventional control movements. For the optimal controller, jet exhaust area (Fig. 7) did not move far from its initial position until the fan stability margin (Fig. 5(c)) had begun to increase (about 1.1 sec into the transient). At that time, jet exhaust area decreased rapidly to its bottom position limit, and this was followed by a rapid increase to its final steady-state value. With the conventional controller, exhaust area increased rapidly, remained constant, and then decreased to its steady-state value (Fig. 7). Fan inlet guide vanes, under optimal control, led the programmed steady-state schedule*, but they lagged the steady-state schedule with the conventional controller (Fig. 9). These differences between the way in which optimal and conventional controllers change the F401 variable engine geometries are similar to those previously reported for high-thrust (80 to 100 percent) engine accelerations (Ref. 2).

Finally, engine fuel flow input for the optimal controller was much more rapid than for the conventional controller (Fig. 8). This difference in engine fuel flow resulted in the more rapid temperature response of the optimal system which was described previously (Fig. 5(a)). The optimal controller was able to rapidly input fuel flow, but, by the proper coordination of all engine controls, avoid overtemperature and stability problems.

*The steady-state schedule adjusts fan and compressor vane position with fan and compressor speeds, respectively, to insure efficient steady-state engine operation.

SYNTHESIS OF AN OPTIMAL INTEGRATED INLET-ENGINE FEEDBACK CONTROL SYSTEM

In this section the design of an integrated feedback controller for the F401 turbofan engine model and an internal compression supersonic inlet model is described. The design objectives and conditions are described initially. Inlet-engine input, state and output variables appropriate for synthesizing feedback control are defined next, and the coupling of inlet-engine dynamics is discussed. The linear optimal control methods used to compute feedback gains are then outlined, and, finally, propulsion system response to simulated afterburner ignition for integrated and separate inlet and engine controllers is compared.

Design Objectives and Conditions

The objective of this effort was to design an integrated controller which uses cross-coupling feedback paths between the inlet and the engine to provide improved inlet-engine dynamic performance. Linear optimization methods were used to compute integrated control gains, and also to compute the inlet control and engine control gains separately. The latter results were used to provide comparative inlet-engine response for non-integrated controls. Design criteria upon which control synthesis was based were (1) regulating the inlet normal shock position, (2) regulating the throat Mach number, and (3) maintaining smooth fan airflow. In addition, the control designs were to allow only small variations in engine stability margins and high turbine inlet temperature so as to insure safe closed-loop system response. The effectiveness of the controllers in satisfying these design criteria was evaluated for simulated engine afterburner ignition.

Supersonic Inlet Model

An internal compression supersonic inlet model was selected for this study because this type of inlet provides the greatest potential for improved dynamic performance. The internal compression inlet operates at its greatest efficiency (highest pressure recovery) when the throat Mach number approaches one, and the normal shock is located very near the inlet throat. However, the normal shock will be expelled from the inlet if the normal shock reaches the throat. This phenomenon is termed "inlet unstart" and results in very inefficient pressure recovery as well as distorted airflow to the engine. An integrated inlet-engine controller may result in significantly increased pressure recovery by permitting safe operation closer to the unstart condition.

A mathematical model of an internal compression supersonic inlet linearized about a flight condition of 40,000 ft, Mach 2.2 was constructed by the Hamilton Standard Division of United Aircraft Corporation. This flight condition was chosen because it represents a military-specified operating point at which aircraft/engine performance is evaluated. Inlet compatibility with the F401 engine was achieved by designing the inlet for F401 fan airflow and fan airflow Mach number at the selected flight condition. The linearized inlet model is shown in Fig. 11. The inlet controls selected were throat area (u_{I1}), bypass area (u_{I2}), and fan corrected airflow (u_{I3}). Fan corrected airflow (an output of the engine) is the coupling variable from the engine to the inlet. The outputs of the two integrators in the inlet model (Fig. 11) were defined to be the inlet states, x_{I1} and x_{I2}. The outputs chosen for the inlet were throat Mach number (y_{I1}), normal shock position (y_{I2}), and fan inlet total pressure (y_{I3}).

The A, B, C and D constant matrices of Eq. (1) for the inlet model are given in Table VII. Table VIII lists values of the steady-state inlet and engine parameters at the 40,000 ft, Mach 2.2 design point. For convenience, throat area, fan inlet total pressure, and afterburner fuel flow were normalized to 1.0 at the design flight condition. Also, normalized values of bypass area and normal shock position were defined to be 0.11 and 0.16, respectively, at the design flight condition. These values for bypass area and normal shock position correspond to their actual values when they are expressed in ft^2 and ft, respectively. Note that a variation of -0.16 in the normal shock position represents the inlet unstart condition. Normalization of the other engine parameters was identical to that defined previously in the discussion of the engine controller synthesis.

Identification of Coupled Inlet-Engine Dynamics

Linearized engine dynamics at the 40,000 ft, Mach 2.2 flight condition were identified first as a prelude to interfacing the inlet model of Fig. 11 with the F401 engine model. Engine state variables were as previously defined; however, the engine control vector was augmented by afterburner fuel flow and fan inlet total pressure. Note that perturbed fan inlet total pressure is also an output of the inlet (see Fig. 11); hence, it represents the coupling variable from the inlet to engine. The engine output variables considered here were thrust, high turbine inlet temperature, fan corrected airflow, fan stability margin, and compressor stability margin. The A, B, C and D constant matrices for this operating point were determined by applying a system identification technique to input-output-state data generated by the F401 computer simulation. Details of the system identification procedure used are contained in Ref. 1. The computed values of the A, B, C and D engine matrices with input, state, and output ordering as defined in this section are presented in Table IX.

The next step in the identification of coupled inlet-engine dynamics was to represent the combined inlet-engine system in the form of Eq. (1). The overall inlet-engine model was formed by combining the previously developed inlet and engine models. The combined inlet-engine states and outputs were the previously defined engine and inlet states and outputs, respectively. Controls for the inlet-engine system consisted of the previously defined inlet and engine controls, with the exception of the coupling variables. Coupling variables represent parameters which are internal to the overall system. The coupling variable from the inlet to the engine was fan inlet total pressure and the coupling variable from the engine to the inlet was fan corrected airflow. The resulting combined system A, B, C and D matrices as well as control, output, and state variable ordering are presented in Table X.

Synthesis of Integrated Inlet-Engine Control

Optimal linear feedback gains were computed by minimizing the performance index

$$J = \frac{1}{2}\int_0^\infty \Big[q_1(T_{IT})^2 + q_2(w_{air})^2 + q_3(CSM)^2 + q_4(CSM)^2 + q_5(N_F)^2 + q_6(N_C)^2 + q_7(M_{TH})^2 + q_8(x_s)^2 + r_1(\dot{A}_j)^2 + r_2(\dot{IGV})^2 + r_3(\dot{RCVV})^2 + r_4(\dot{w}_f)^2 + r_5(\dot{w}_{ab})^2 + r_6(\dot{A}_{TH})^2 + r_7(\dot{A}_{BY})^2 \Big] dt \qquad (5)$$

where q_i, r_i are weighting factors, and

$w_{air} \triangleq$ perturbed fan corrected airflow

$N_F \triangleq$ perturbed fan speed

$N_C \triangleq$ perturbed high compressor speed

$M_{TH} \triangleq$ perturbed throat Mach number

$x_s \triangleq$ perturbed normal shock position

$w_{ab} \triangleq$ perturbed afterburner fuel flow

$A_{TH} \triangleq$ perturbed throat area

$A_{BY} \triangleq$ perturbed bypass area

while the other symbols are as previously defined. The performance index includes all of the input rates to account for and satisfy actuation rate limits. The remaining parameters are included because their response is critical in evaluating closed-loop system performance. The structure of the resulting multivariable controller is shown in Fig. 2(b). Because only the regulator problem was considered ($\delta z = 0$ in Fig. 2(b)), the standard structure of Fig. 2(b) was not transformed to the integral structure of Fig. 2(c).

Before the weighting factors were chosen, acceptable propulsion system response to a simulated afterburner ignition was defined. The design criteria for inlet performance specified that variations in throat Mach number and normal shock position be minimized. For satisfactory engine performance the variations in fan corrected airflow, fan stability margin, compressor stability margin and high turbine inlet temperature were also to be minimized. In addition, the engine was to be maintained near its steady-state operating point since this point represents efficient engine operation for the given flight condition. This was accomplished by permitting only small transient variations in fan and high compressor speeds.

The performance index weightings were selected so that the resulting controller feedback gains produced satisfactory inlet-engine response to a disturbance equivalent to that from an afterburner light. This disturbance consisted of a step change in afterburner fuel flow. A very large weighting factor, r_5, was used to insure that afterburner fuel flow had a negligibly small rate-of-decrease to zero from its stepped value. Table XI lists the set of weightings and Table XII the controller feedback gains for which inlet-engine response will be shown. The integrated controller is comprised of engine feedback gains, inlet feedback gains, and cross-coupling gains between the inlet and engine. The gain matrices (G_1 and G_2, Fig. 2(b)), have therefore been partitioned as

$$G_1 = \left[\begin{array}{c|c} G_{1E} & G_{1EI} \\ \hline G_{1IE} & G_{1I} \end{array}\right] \qquad G_2 = \left[\begin{array}{c|c} G_{2E} & G_{2EI} \\ \hline G_{2IE} & G_{2I} \end{array}\right] \tag{6}$$

The 5 x 5 G_{1E} and G_{2E} matrices represent feedback paths to engine control rates from engine states and control inputs, respectively. The feedback gains to inlet control rates from inlet states and controls are given by the 2 x 2 gain matrices G_{1I} and G_{2I}, respectively. The 5 x 2 gain matrices G_{1EI} and G_{2EI} represent the coupling gains from the inlet states and controls, respectively, to the engine control rates. The coupling gains from the engine states and controls to the inlet control rates are the 2 x 5 gain matrices G_{1IE} and G_{2IE}, respectively.

Synthesis of Separate Inlet and Engine Controllers

Separate inlet and engine controllers were also designed using modern control theory. The separate inlet controller used only inlet information to achieve satisfactory inlet performance, and the separate engine control used only engine information. Designing the engine and inlet controls separately ignored the known cross-coupling between engine and inlet variables. However, there was no specification that a particular control variable was to control a particular output variable. Cross-coupling paths within the engine alone and within the inlet alone were used.

Feedback gains for the inlet control were computed by minimizing

$$J = \frac{1}{2}\int_0^\infty \left[q_7(M_{TH})^2 + q_8(x_s)^2 + r_6(\dot{A}_{TH})^2 + r_7(\dot{A}_{BY})^2 + r_8(w_{air})^2 \right] dt \qquad (7)$$

and the gains for the engine control were computed by minimizing

$$J = \frac{1}{2}\int_0^\infty \left[q_1(T_{IT})^2 + q_2(w_{air})^2 + q_3(FSM)^2 + q_4(CSM)^2 + q_5(N_F)^2 + q_6(N_C)^2 \right. \\ \left. + r_1(\dot{A}_j)^2 + r_2(\dot{IGV})^2 + r_3(\dot{RCVV})^2 + r_4(\dot{w}_f)^2 + r_5(\dot{w}_{ab})^2 \right] dt \qquad (8)$$

where the symbols are as previously defined. Recall that for the inlet model alone, perturbed fan corrected airflow was considered an input (see Fig. 11). The control optimization procedure therefore theoretically called for direct fan airflow control to regulate the inlet. However, this is inconsistent with propulsion system design. That is, fan airflow can only be controlled indirectly, e.g., by changing system geometries or fuel flows. To reconcile the model mathematics with the actual propulsion system, a very large weighting, r_8, on perturbed airflow was used. The large weighting resulted in negligibly small feedback gains to airflow and thereby avoided the implications of direct airflow control.

Weighting factors were chosen for the performance indices of Eqs. (7) and (8) which were identical to the weighting factors in the integrated control performance index of Eq. (5). The gain matrices G_1 and G_2 for the inlet and engine models, when the inlet controller and engine controller were designed separately, are given in Table XIII. Note that the gain matrices resulting from separate engine and inlet control synthesis are approximately the same as the integrated control gain matrices (Table XII), except that the inlet-engine cross-coupling feedbacks are zero for separate control synthesis.

Comparison of Inlet-Engine Response with Separate and Integrated Controllers

Inlet-engine model response with the integrated controller was calculated for a simulated afterburner ignition consisting of a 10-percent step in afterburner fuel flow. The effects of this step are considered to be representative of the disturbances caused by afterburner lightoff. The closed-loop time responses for the integrated controller are shown in Fig. 12. For the given step in afterburner fuel flow, a 6-percent increase in steady-state thrust resulted with less than 1-percent maximum variation in fan stability margin and less than 0.5-percent maximum variation in fan corrected airflow, compressor stability margin and high turbine inlet temperature. The changes in the steady-state values of the fan and high compressor speeds caused by simulated afterburner ignition were negligible. The maximum variation in throat Mach number was less than 0.002 and the maximum variation in normal shock position was 0.0053.

Comparative closed-loop time responses are also shown in Fig. 12 for the controller which had been designed by considering the engine and inlet separately. The engine performance remained essentially unchanged from that which resulted for integrated control. There was a minor improvement in throat Mach number variation; however, the maximum variation in normal shock position more than tripled from -0.0017 for integrated control to -0.0053 for separate control (recall that a variation of -0.16 would cause inlet unstart). This tripling of the normal shock position variation represents a significant deterioration in dynamic performance due to separate inlet and engine control. These results also imply that for integrated control it may be possible to operate closer to the inlet unstart condition and thereby achieve greater inlet pressure recovery.

As noted before, the gains of the integrated controller are very similar to the gains of the separate inlet and engine controllers, except that the integrated controller contains inlet-engine cross-coupling terms. To obtain further insight into the influence of these cross-coupling terms, the inlet-engine model response was calculated for the integrated controller with cross-coupling gains zeroed. Results showed that inlet-engine performance with the cross-coupling terms removed from the integrated controller was almost identical to system performance with the separately designed controller. This indicates that the improved inlet performance with the integrated control was a direct result of the cross-coupling feedback gains.

To determine whether a controller without inlet-engine cross-coupling gains could be designed to perform as well as the integrated controller, the normal shock position weighting, q_8, in the inlet control performance index (Eq. (7)) was increased. Recall that it was the normal shock whose response deteriorated the most with the separate controllers. As the change in inlet normal shock position was penalized more heavily, the observed variation in normal shock position for the

separate controllers decreased, but the variation in throat Mach number increased. The engine response remained essentially unchanged. When the weighting (q_8) was increased to the point where the throat Mach number variation was the same as that for the integrated control (recall that it had been less for the separate controls with the original q_8 weighting), the normal shock position variation was approximately double that of the integrated control. The weighting was then further increased until the variation in normal shock position was essentially the same as that for the integrated control. Inlet response for this controller is compared with inlet response for the previously developed integrated controller in Fig. 15. The throat Mach number variation is six times larger with the separately designed controller than with the integrated controller. The bypass area excursion also increased by a factor of four while the throat area excursion increased by a factor of six. Both inlet actuators were required to move twice as fast with the separate controllers as with the integrated controller. Because the engine control remains unchanged, and the computed inlet variations due to the afterburner ignition have little effect on the engine, the engine response was identical to that presented in Fig. 12. The inlet weighting factors and inlet gain matrices (G_{1I} and G_{2I}) for this high q_8 weighting controller ($q_8 = 50{,}000$) are shown in Table XIV. The engine control was not changed so that its parameters remain as given in Table XIII.

The results discussed here demonstrate that inlet response to an afterburner ignition can be improved by an integrated controller. The optimal control theory identified fan corrected airflow as a coupling variable and defined cross-coupling gains to provide improved inlet regulation of the effects of a downstream disturbance. The cross-coupling feedbacks from engine to inlet modulated the inlet controls so as to maintain normal shock position with a smaller variation in throat Mach number and less control effort than the separately designed controller. The engine response to inlet distortion was not investigated. However, the computed coupling gains from the inlet to engine verify that the fan inlet total pressure coupling variable was identified by the control synthesis procedure. These gains could be used to modulate the engine inputs and improve engine performance to an upstream disturbance.

CURRENT UARL PROGRAM

The current UARL program sponsored by ONR is focused on the development of parameter identification and adaptive control for advanced technology propulsion systems*. Identification of engine parameters is the key to applying the control optimization method described in this report to a real rather than simulated engine. That is, the piecewise-linear/piecewise-optimal approach to multivariable control synthesis requires that the engine stability and control derivatives be known (A, B, C and D matrices). Accurate determination of turbofan engine stability and control parameters is difficult, because (1) not all engine variables can be sensed, (2) data from sensed engine variables are noise-corrupted, and (3) the parameter values change with altitude, Mach number, and power lever angle. Algorithms which account for these difficulties and provide valid estimates of the engine dynamics are currently not available.

Modern (optimal) filtering methods are applicable to realistic jet engine estimation problems, e.g., operation on noise-corrupted engine input-output data and incomplete sensing of engine variables. Optimal filtering theory is being employed in the current UARL studies to estimate those parameters which are critical in assessing engine performance. Also, on-line computation of engine parameters provides the data necessary to develop and implement a self-adaptive control algorithm which would optimize propulsion system performance in flight. The feasibility of using these newly estimated parameters as the basis for on-line adaptive control optimization will be evaluated in the UARL program. An algorithm for adaptive engine performance control will be developed using thrust specific fuel consumption as the performance criterion for the optimization process.

*In a related program being funded by P&WA, UARL and P&WA engineers are evaluating hardware and software requirements involved in implementing the optimal multivariable controllers developed under ONR sponsorship. A PDP-11 digital computer is being coded to simulate the optimal multivariable controller in real time. An F401 engine model, defined by the parameters of Tables II and III, is being programmed on a Beckman analog computer. The resulting real-time hybrid simulation will be used (1) to study system accuracy and closed-loop stability, (2) to investigate digital control cycle time requirements, and (3) to resolve interface problems associated with a discrete controller and a continuous F401 engine.

REFERENCES

1. Michael, G. J. and F. A. Farrar: An Analytical Method for the Synthesis of Nonlinear Multivariable Feedback Control. United Aircraft Research Laboratories Report M941338-2, prepared under Department of the Navy Contract N00014-72-C-0414, June 1973 (DDC Accession Number AD 762797).

2. Michael, G. J. and F. A. Farrar: Development of Optimal Control Modes for Advanced Technology Propulsion Systems. United Aircraft Research Laboratories Report M911620-1, prepared under Department of the Navy Contract N00014-73-C-0281, August 1973 (DDC Accession Number AD 767425).

3. Anon.: F100-PW-100 (F100/F401) Digital Dynamic Simulation User's Manual for Deck CCD 1015-3.2, Book 1 of 2. Pratt & Whitney Aircraft Report PWA FR-3794B, prepared under Department of the Air Force Contract F33657-70-C-0600, 15 October 1970, revised 25 April 1972.

4. Athans, M. and P. L. Falb: Optimal Control. McGraw Hill Book Company, New York, 1966.

LIST OF SYMBOLS

A	Constant n x n matrix used to describe linearized system dynamics
A_{BY}	Perturbed bypass area, normalized
A_j	Perturbed jet exhaust area, normalized
A_{TH}	Perturbed throat area, normalized
B	Constant n x m matrix used to describe linearized system dynamics
C	Constant p x n matrix used to describe linearized system dynamics
CSM	Perturbed compressor stability margin, normalized
D	Constant p x m matrix used to describe linearized system dynamics
deg	Degrees
E	Constant 4 x 7 matrix relating system output to commanded output
F	Perturbed thrust, normalized
FSM	Perturbed fan stability margin, normalized
G	Standard optimal closed-loop feedback gain matrix
G_1	m x n partition of the matrix G
G_{1E}	5 x 5 partition of the inlet-engine gain matrix G_1
G_{1EI}	5 x 2 partition of the inlet-engine gain matrix G_1
G_{1I}	2 x 2 partition of the inlet-engine gain matrix G_1
G_{1IE}	2 x 5 partition of the inlet-engine gain matrix G_1
G_2	m x m partition of the matrix G
G_{2E}	5 x 5 partition of the inlet-engine gain matrix G_2
G_{2EI}	5 x 2 partition of the inlet-engine gain matrix G_2

LIST OF SYMBOLS (Continued)

G_{2I}	2 x 2 partition of the inlet-engine gain matrix G_2
G_{2IE}	2 x 5 partition of the inlet-engine gain matrix G_2
H	4 x 4 optimal integral feedback gain matrix
IGV	Perturbed fan inlet guide vanes, normalized
i	General subscript
J	Performance index
L	4 x 5 optimal integral feedback gain matrix
M	m x m feedforward gain matrix
m	Dimension of system control vector u
M_{TH}	Perturbed throat Mach number
N_C	Perturbed high compressor speed, normalized
N_F	Perturbed fan speed, normalized
N_1	Fan speed, normalized
N_2	High compressor speed, normalized
n	Dimension of system state vector x
PLA	Power-lever angle
p	Dimension of system output vector y
q_i	Performance index weighting factor --- a scalar
RCVV	Perturbed rear compressor variable vanes, normalized
r_i	Performance index weighting factor --- a scalar
T_{IT}	Perturbed high turbine inlet temperature, normalized

LIST OF SYMBOLS (Continued)

t	Time, sec
u	m x 1 control vector
u^*	m x 1 optimal control vector
u_i	i^{th} component of u
u_{Ij}	j^{th} inlet control variable
v	4 x 1 vector consisting of those elements of the output vector y whose steady-state values it is desired to specify
v_i	i^{th} component of v
w	m x 1 control rate vector --- w = du/dt
w_{ab}	Perturbed afterburner fuel flow, normalized
w_{air}	Perturbed fan airflow, normalized
w_f	Perturbed main burner fuel flow, normalized
x	n x 1 state vector
x_i	i^{th} component of x
x_s	Perturbed normal shock position, normalized
x_{Ij}	j^{th} inlet state variable
y	p x 1 output vector
y_i	i^{th} component of y
y_{Ij}	j^{th} inlet output variable
z	m x 1 command input vector
z_i	i^{th} component of z

LIST OF SYMBOLS (Concluded)

τ	Variable of integration
$(\dot{})$	Time derivative of the quantity in parentheses
$d(\ )$	Differential of the quantity in parentheses
$\delta(\ )$	Perturbational value of the quantity in parentheses
$\triangleq$	Equals by definition

TABLE I

NORMALIZED STEADY-STATE ENGINE PARAMETERS
AS A FUNCTION OF POWER LEVER ANGLE

Engine Parameters		Power Lever Angle, PLA-deg				
Type	Parameter	20	35	47	60	73
Output	Thrust	0.09	0.35	0.52	0.72	1.0
	High Turbine Inlet Temperature	0.56	0.73	0.81	0.90	1.0
	Fan Airflow	0.34	0.62	0.73	0.85	1.0
	Fan Stability Margin	0.10	0.14	0.18	0.12	0.12
	Compressor Stability Margin	0.16	0.18	0.18	0.19	0.19
State	Fan Turbine Inlet Temperature	0.57	0.72	0.81	0.90	1.0
	Main Burner Pressure	0.21	0.45	0.59	0.77	1.0
	Fan Speed	0.49	0.74	0.83	0.91	1.0
	High Compressor Speed	0.69	0.83	0.88	0.93	1.0
	Afterburner Pressure	0.40	0.55	0.66	0.82	1.0
Control	Jet Exhaust Area	0.98	0.98	0.98	0.98	1.0
	Fan Inlet Guide Vanes	-0.50	-0.50	-0.50	-0.34	-0.08
	Rear Compressor Variable Vanes	-1.11	-0.39	-0.17	0.04	0.20
	Main Burner Fuel Flow	0.12	0.33	0.48	0.70	1.0

TABLE II

IDENTIFIED VALUES OF LINEARIZED ENGINE DYNAMICS -
A AND B MATRICES AS A FUNCTION OF POWER LEVER ANGLE

PLA-deg	Matrix	Matrix Elements				
20	A	-56.450	19.387	2.403	-48.947	17.867
		8.066	-71.982	2.184	47.511	-1.2[illegible]4
		0.123	4.135	-1.672	-0.500	-2.463
		0.222	3.912	-0.098	-2.791	-0.514
		-0.877	5.472	1.309	-2.938	-9.303
	B	0.626	0.005	-1.247	103.080	
		-0.183	0.001	1.362	3.300	
		-0.011	-0.085	-0.011	0.030	
		0.004	0.003	-0.097	-0.131	
		-0.917	0.017	-0.147	0.198	
35	A	-64.848	12.421	-15.113	-36.828	2.202
		23.201	-68.809	24.036	66.740	7.405
		0.448	4.983	-2.911	-0.766	-2.742
		1.253	2.071	-0.473	-2.881	-0.777
		-1.720	7.956	-0.538	-3.743	-7.617
	B	0.808	-0.144	-4.129	56.602	
		0.020	0.260	5.866	-2.124	
		-0.063	-0.132	-0.055	-0.316	
		-0.074	-0.011	-0.180	-0.733	
		-2.856	-0.258	-0.589	-0.397	
47	A	-57.096	3.613	-10.211	-5.481	-2.715
		19.832	-72.340	30.295	40.972	15.327
		0.660	4.496	-3.601	-0.011	-2.808
		1.326	2.313	-0.809	-3.032	-0.821
		0.882	0.703	2.922	1.471	-4.596
	B	1.017	-0.553	-3.941	39.792	
		-0.125	1.416	7.888	4.181	
		-0.077	-0.316	-0.031	-0.382	
		-0.088	-0.033	-0.253	-0.565	
		-3.563	-0.149	-0.097	-0.785	

(Continued)

TABLE II (Concluded)

PLA-deg	Matrix	Matrix Elements				
60	A	-39.255	-21.855	4.762	8.122	4.711
		-3.034	-31.287	9.385	15.460	4.615
		0.798	4.729	-3.880	-0.156	-3.095
		1.539	1.991	-0.828	-2.524	-0.817
		0.425	-2.882	4.688	3.235	-3.436
	B	2.017	0.370	-0.273	27.141	
		-1.572	0.598	4.171	9.866	
		-0.145	-0.394	-0.036	-0.362	
		-0.120	-0.065	-0.367	-0.513	
		-4.471	-0.069	0.339	0.396	
73	A	-34.013	-9.303	12.037	-2.398	-1.254
		4.389	-38.762	-4.221	28.480	14.729
		-4.755	2.287	-0.400	-1.546	-2.200
		2.046	1.062	-0.729	-2.150	-0.624
		4.151	-8.814	-0.167	7.477	1.099
	B	0.766	0.546	-0.813	17.095	
		0.056	1.341	7.737	8.641	
		0.156	-1.176	-0.416	2.034	
		-0.137	-0.024	-0.55[illegible]	-0.378	
		-4.729	0.874	1.617	0.223	

TABLE III

IDENTIFIED VALUES OF LINEARIZED ENGINE DYNAMICS -
C AND D MATRICES AS A FUNCTION OF POWER LEVER ANGLE

PLA-deg	Matrix	Matrix Elements				
20	C	0	0	0	0	0
		0	0	0	0	0
		-0.006	-0.025	-0.013	0.002	2.118
		1.057	0.471	-0.028	-0.028	-0.228
		-0.023	0.075	1.103	-0.030	-0.304
		-0.053	0.314	0.329	-0.109	-1.546
		-0.244	-4.114	-0.026	4.415	-0.023
	D	0	1.0	0	0	
		0	0	1.0	0	
		0.095	-0.002	0	0.009	
		-0.004	0.001	-0.003	-0.183	
		-0.003	0.079	-0.002	0.012	
		-0.022	0.046	-0.004	0.021	
		-0.007	-0.005	0.001	0.222	
35	C	0	0	0	0	0
		0	0	0	0	0
		-0.003	-0.031	0.001	0.008	1.618
		1.064	0.231	-0.061	-0.031	-0.129
		-0.035	0.161	1.114	-0.003	-0.386
		-0.101	0.663	1.443	-0.065	-1.562
		0.013	-1.624	0.602	2.218	0.238
	D	0	1.0	0	0	
		0	0	1.0	0	
		0.372	0	0.001	0.007	
		-0.011	-0.002	-0.005	-0.105	
		-0.023	0.068	0.002	0.008	
		-0.081	0.133	0.020	0.041	
		0.007	0.009	0.121	-0.038	
47	C	0	0	0	0	0
		0	0	0	0	0
		-0.037	0.031	-0.016	-0.042	1.368
		1.081	0.149	-0.057	0.001	-0.086
		-0.006	0.098	1.298	-0.014	-0.236
		-0.053	0.241	0.339	0.076	-0.925
		-0.250	-1.154	0.415	1.751	0.226

(Continued)

TABLE VII (Concluded)

PIA-deg	Matrix	Matrix Elements				
47	D	0	1.0	0	0	
		0	0	1.0	0	
		0.546	0.003	-0.005	0.018	
		-0.013	-0.002	0	-0.086	
		-0.026	0.152	0.004	0.009	
		-0.077	0.078	0.018	0.021	
		-0.007	0.018	0.108	0.116	
60	C	0	0	0	0	0
		0	0	0	0	0
		-0.020	0.037	-0.005	-0.025	1.357
		1.059	0.119	-0.051	0	-0.066
		-0.016	0.032	1.479	0.025	-0.136
		-0.151	0.124	0.314	0.120	-0.780
		-0.847	-0.109	-0.126	1.456	-0.119
	D	0	1.0	0	0	
		0	0	1.0	0	
		0.783	0.003	-0.006	0.002	
		-0.015	-0.003	-0.004	-0.064	
		-0.016	0.192	0.007	0.009	
		-0.063	0.064	0.020	0.064	
		-0.047	-0.012	0.024	0.252	
73	C	0	0	0	0	0
		0	0	0	0	0
		-0.042	0.063	0.013	-0.054	1.404
		1.045	0.092	-0.060	-0.028	-0.050
		0.386	0.100	-0.217	0.170	-0.095
		0.305	-0.326	-0.458	0.584	-0.538
		-0.183	-0.564	0.394	-0.165	0.394
	D	0	1.0	0	0	
		0	0	1.0	0	
		1.044	0.001	-0.013	0.002	
		-0.015	-0.003	-0.013	-0.044	
		-0.043	0.278	0.035	-0.155	
		-0.101	0.281	0.137	-0.041	
		0.073	0.047	-0.091	0.050	

TABLE IV

NORMALIZED POSITION AND RATE
LIMITS FOR ENGINE CONTROLS

Controls	Normalized Limits		
	Rate Limits	Upper Position Limit	Lower Position Limit
Jet Exhaust Area	± 1.28	2.3	0.8
Fan Inlet Guide Vanes	± 1.25	0	-0.5
Rear Compressor Variable Vanes	± 5.00	0.2	-2.0
Main Burner Fuel Flow	± 1.76	1.2	0.1

TABLE V

PERFORMANCE INDEX WEIGHTING FACTORS FOR DESIGN OF OPTIMAL MULTIVARIABLE ENGINE CONTROLLER

Performance Index and Weighting Factors of Eq. (3)

Power Lever Angle, PLA-deg	Output Weighting Factors						Control Weighting Factors			
	q_1	q_2	q_3	q_4	q_5	q_6	r_1	r_2	r_3	r_4
20	160	40	10	2500	0	2000	5000	16	500	5
35	160	40	10	5000	0	100	1000	16	100	5
47	160	40	500	40000	640	0	25	16	1	5
60	160	40	500	20000	640	0	25	16	1	5
73	160	40	1000	500	0	0	160	16	1	9

$q_1 \triangleq$ weighting on perturbed fan inlet guide vanes

$q_2 \triangleq$ weighting on perturbed rear compressor variable vanes

$q_3 \triangleq$ weighting on perturbed thrust

$q_4 \triangleq$ weighting on perturbed high turbine inlet temperature

$q_5 \triangleq$ weighting on rate-of-change of fan stability margin

$q_6 \triangleq$ weighting on rate-of-change of high compressor stability margin

$r_1 \triangleq$ weighting on rate-of-change of exhaust area

$r_2 \triangleq$ weighting on rate-of-change of fan inlet guide vanes

$r_3 \triangleq$ weighting on rate-of-change of rear compressor variable vanes

$r_4 \triangleq$ weighting on rate-of-change of fuel flow

TABLE VI

FEEDBACK GAIN H AND L MATRICES FOR
OPTIMAL MULTIVARIABLE ENGINE CONTROLLER

Intermediate Values of H and L Scheduled
Linearly with High Compressor Speed, N_2

Power Lever Angle, PLA-deg	N_2	Matrix	Matrix Elements				
20	0.69	H	0.001	0.001	0.073	-0.057	
			-3.144	-0.024	0.002	-1.307	
			0.003	-0.282	-0.006	0.220	
			0.064	-0.057	0.012	-4.930	
		L	-0.001	-0.006	0.013	0.046	0.011
			-0.346	-3.457	0.122	1.699	0.055
			-0.046	-0.494	-0.037	0.907	-0.018
			-1.447	-7.308	0.207	3.635	0.107
35	0.83	H	-0.027	0.017	-0.481	0.685	
			-3.161	0.002	0.019	0.064	
			0	-0.627	-0.022	0.283	
			-0.037	-0.163	0.124	-31.369	
		L	-0.007	-0.027	-0.121	-0.452	-0.052
			-0.004	0.047	-0.013	-0.038	-0.004
			-0.010	0.091	-0.037	-0.094	-0.018
			-0.801	-2.518	1.101	2.756	0.518
47	0.88	H	0.826	0.505	3.578	-2.175	
			-2.554	0.086	2.497	0.457	
			4.252	-4.777	8.690	37.490	
			0.467	-0.293	0.223	-87.033	
		L	-0.001	0.209	0.494	1.063	2.302
			0.151	-0.359	-0.015	0.752	2.156
			1.254	-2.308	-2.333	3.453	14.077
			-1.187	-0.523	-0.124	0.276	1.860

(Continued)

TABLE VI (Concluded)

Power Lever Angle, PLA-deg	N_2	Matrix	Matrix Elements				
60	0.93	H	0.836	0.280	3.736	-6.991	
			-2.680	0.058	2.482	2.685	
			3.319	-5.106	6.819	35.689	
			0.230	-0.201	-0.811	-54.422	
		L	-0.072	-0.185	0.752	1.309	2.617
			0.297	-0.143	0.033	0.592	1.701
			2.372	-3.665	-2.029	2.866	11.213
			-0.902	0.237	-0.472	-0.258	0.690
73	1.0	H	-0.068	0.252	2.070	-0.416	
			-3.143	0.056	-0.674	0.347	
			-0.908	-5.350	16.616	1.255	
			-0.217	-0.357	-1.855	-7.218	
		L	0.029	-0.185	0.499	0.322	0.962
			-0.005	0.009	0.107	-0.009	-0.038
			0.363	-1.163	1.864	1.234	5.684
			-0.155	0.095	-0.815	0.034	-0.535

TABLE VII

LINEARIZED INLET DYNAMICS
AT 40,000 FT, MACH 2.2 OPERATING CONDITION

Matrix	Matrix Elements		
A	-100.00 236.40	0 -37.04	
B	0 -427.20	30.00 0	136.89 0
C	0 -0.18 0.03	0 1.00 -0.16	
D	-2.52 2.41 0.14	0 0 0	0 0 0

State Ordering	Control Ordering	Output Ordering
Inlet state 1 (see Fig. 11) Inlet state 2 (see Fig. 11)	Throat area Bypass area Fan corrected airflow	Throat Mach number Normal shock position Fan inlet total pressure

TABLE VIII

NORMALIZED STEADY-STATE INLET-ENGINE PARAMETERS
AT 40,000 FT, MACH 2.2 OPERATING CONDITION

Parameter Type	Parameter Name	Normalized Value
Output	Thrust	1.48
	High Turbine Inlet Temperature	1.07
	Fan Corrected Airflow	0.71
	Fan Stability Margin	0.23
	Compressor Stability Margin	0.19
	Throat Mach Number	1.30
	Inlet Normal Shock Position	0.16
	Fan Inlet Total Pressure	1.0
State	Fan Turbine Inlet Temperature	1.08
	Main Burner Pressure	0.88
	Fan Speed	0.97
	High Compressor Speed	1.03
	Afterburner Pressure	0.91
Control	Jet Exhaust Area	1.83
	Fan Inlet Guide Vanes	-0.50
	Rear Compressor Variable Vanes	-0.34
	Main Burner Fuel Flow	0.85
	Afterburner Fuel Flow	1.0
	Throat Area	1.0
	Bypass Area	0.11

TABLE IX

LINEARIZED ENGINE DYNAMICS
AT 40,000 FT, MACH 2.2 OPERATING CONDITION

PLA = 120 deg

Matrix	Matrix Elements					
A	-55.478	2.640	-5.583	-13.881	0.651	
	27.172	-93.200	48.331	117.200	11.393	
	0.801	4.783	-5.872	-0.351	-2.824	
	2.146	1.636	-0.656	-3.967	-0.560	
	3.148	0.354	7.076	2.516	-8.539	
B	0.500	-0.417	-3.085	28.630	0	-21.883
	-0.806	1.214	12.911	4.734	-0.260	63.993
	-0.074	-0.326	-0.006	-0.275	-0.045	-1.154
	-0.080	-0.026	-0.270	-0.755	-0.015	-0.310
	-4.362	0.583	0.326	-1.237	1.946	6.195
C	0.001	-0.007	-1.840	-0.131	3.405	
	1.128	0.073	-0.050	0.064	-0.058	
	0.011	-0.015	1.168	0.102	-0.092	
	0.093	-0.081	0.658	0.639	-0.429	
	-0.210	-0.687	0.388	1.451	0.115	
D	1.481	-0.144	-0.017	-0.008	0.004	-1.270
	-0.009	0.001	0.008	-0.086	0	0.061
	-0.007	0.091	0.014	0.004	-0.002	0.108
	-0.031	0.078	0.079	0.001	-0.027	0.523
	0.004	0.018	0.075	0.063	0.006	0.439

State Ordering	Control Ordering	Output Ordering
Fan turbine inlet temperature	Jet exhaust area	Thrust
Main burner pressure	Fan inlet guide vanes	High turbine inlet temperature
Fan speed	Rear compressor variable vanes	Fan corrected airflow
High compressor speed	Main burner fuel flow	Fan stability margin
Afterburner pressure	Afterburner fuel flow	Compressor stability margin
	Fan inlet total pressure	

TABLE X

LINEARIZED INLET-ENGINE DYNAMICS
AT 40,000 FT, MACH 2.2 OPERATING CONDITION

Matrix	Matrix Elements						
A	-55.478	-2.640	-5.583	-13.881	0.651	-0.643	3.501
	27.172	-93.200	48.331	117.200	11.393	1.881	-10.239
	0.801	4.783	-5.872	-0.351	-2.824	-0.034	0.185
	2.146	1.636	-0.656	-3.967	-0.560	-0.009	0.050
	3.148	0.354	7.076	2.516	-8.539	0.182	-0.991
	1.445	-2.120	159.940	14.024	-12.610	-99.565	-2.370
	0	0	0	0	0	236.400	-37.040
B	0.500	-.417	-3.085	28.630	0	-3.092	0
	-0.806	1.214	12.911	4.734	-0.260	9.044	0
	-0.074	-0.326	-0.006	-0.275	-0.045	-0.163	0
	-0.080	-0.026	-0.270	-0.755	-0.015	-0.044	0
	-4.362	0.583	0.326	-1.237	1.946	0.875	0
	-1.024	12.512	1.870	0.501	-0.338	2.093	30.000
	0	0	0	0	0	-427.200	0
C	0.001	-0.007	-1.840	-0.131	3.405	-0.037	0.203
	1.128	0.073	-0.050	0.064	-0.058	0.002	-0.010
	0.011	-0.015	1.168	0.102	-0.092	0.003	-0.017
	0.093	-0.081	0.658	0.639	-0.429	0.015	-0.084
	-0.210	-0.687	0.388	1.451	0.115	0.013	-0.070
	0	0	0	0	0	0	0
	0	0	0	0	0	-0.184	1.000
	0	0	0	0	0	0.029	-0.160
D	1.481	-0.144	-0.017	-0.008	0.004	-0.180	0
	-0.009	0.001	0.008	-0.086	0	0.009	0
	-0.007	0.091	0.014	0.004	-0.002	0.015	0
	-0.031	0.078	0.079	0.001	-0.027	0.074	0
	0.004	0.018	0.075	0.063	0.006	0.062	0
	0	0	0	0	0	-2.520	0
	0	0	0	0	0	2.413	0
	0	0	0	0	0	0.141	0

(Continued)

TABLE X (Concluded)

State Ordering	Control Ordering	Output Ordering
Fan turbine inlet temperature	Jet exhaust area	Thrust
Main burner pressure	Fan inlet guide vanes	High turbine inlet temperature
Fan speed	Rear compressor variable vanes	Fan corrected airflow
High compressor speed	Main burner fuel flow	Fan stability margin
Afterburner pressure	Afterburner fuel flow	Compressor stability margin
Inlet state 1 (see Fig. 11)	Throat area	Throat Mach number
Inlet state 2 (see Fig. 11)	Bypass area	Normal shock position
		Fan inlet total pressure

TABLE XI

PERFORMANCE INDEX WEIGHTING FACTORS FOR
DESIGN OF INLET-ENGINE CONTROLLERS

Weighting Factor	Perturbed Parameter Weighted	Value
q_1	High Turbine Inlet Temperature	500
q_2	Fan Corrected Airflow	6400
q_3	Fan Stability Margin	100
q_4	Compressor Stability Margin	200
q_5	Fan Speed	500
q_6	High Compressor Speed	250
q_7	Throat Mach Number	100
q_8	Normal Shock Position	100
r_1	Rate-of-Change of Exhaust Area	15
r_2	Rate-of-Change of Fan Inlet Guide Vanes	16
r_3	Rate-of-Change of Rear Compressor Variable Vanes	1
r_4	Rate-of-Change of Main Burner Fuel Flow	8
r_5	Rate-of-Change of Afterburner Fuel Flow	10^5
r_6	Rate-of-Change of Throat Area	22
r_7	Rate-of-Change of Bypass Area	2
r_8	Fan Corrected Airflow (Inlet Control Design Only)	10^7

TABLE XII

FEEDBACK GAIN MATRICES G_1 AND G_2 OF THE INTEGRATED INLET-ENGINE CONTROLLER FOR WEIGHTINGS SHOWN IN TABLE XI

Matrix	Matrix Elements						
G_1	-0.185	-0.151	-1.826	-3.341	0.832	-0.012	-0.007
	-0.137	-0.189	-3.946	-1.240	0.740	-0.054	-0.012
	-1.844	-2.190	-36.135	-27.566	10.438	-0.130	-0.033
	-0.736	-0.473	-6.995	-7.335	2.566	-0.094	-0.044
	0	0	0	0	0	0	0
	0.221	0.266	6.092	1.268	-0.907	0.768	0.215
	-0.712	-0.941	-19.702	-6.188	3.484	-1.543	-0.479
G_2	-1.579	-0.093	-0.350	-1.034	1.021	0.189	[illegible]
	[illegible]	[illegible]	[illegible]	[illegible]	[illegible]	0.659	[illegible]
	-5.245	-2.350	-4.516	-4.535	3.541	2.768	-1.397
	-1.939	-0.392	-0.567	-5.734	1.257	1.499	-0.301
	0	0	0	0	0	0	0
	0.129	0.480	0.126	0.545	-0.127	-13.872	1.964
	-0.580	-1.565	-0.699	-1.206	0.537	21.602	-6.964

TABLE XIII

FEEDBACK GAIN MATRICES G_1 AND G_2 OF THE SEPARATE INLET-ENGINE CONTROLLERS FOR WEIGHTINGS SHOWN IN TABLE XI

Matrix	Matrix Elements						
G_1	-0.179	-0.144	-1.679	-3.266	0.797	0	0
	-0.113	-0.156	-3.230	-1.079	0.628	0	0
	-1.692	-1.996	-32.509	-26.146	9.682	0	0
	-0.693	-0.417	-5.871	-6.888	2.338	0	0
	0	0	0	0	0	0	0
	0	0	0	0	0	0.870	0.258
	0	0	0	0	0	-1.741	-0.570
G_2	-1.575	-0.082	-0.340	-1.018	1.018	0	0
	-0.077	-0.674	-0.129	-0.152	0.080	0	0
	-5.107	-2.065	-4.362	-4.104	3.421	0	0
	-1.908	-0.304	-0.513	-5.680	1.226	0	0
	0	0	0	0	0	0	0
	0	0	0	0	0	-14.984	2.167
	0	0	0	0	0	23.838	-7.266

TABLE XIV

FEEDBACK GAIN MATRICES G_{1I} AND G_{2I} FOR INLET CONTROL WITH INCREASED PERFORMANCE INDEX WEIGHTING ON NORMAL SHOCK POSITION

Matrix	Matrix Elements	
G_{1I}	53.494 -106.880	15.752 -59.405
G_{2I}	-148.420 224.280	20.389 -42.391

N911620-2

SCHEDULES OF NORMALIZED STEADY STATE ENGINE PARAMETERS AS A FUNCTION OF POWER LEVER ANGLE FOR F401 TURBOFAN ENGINE

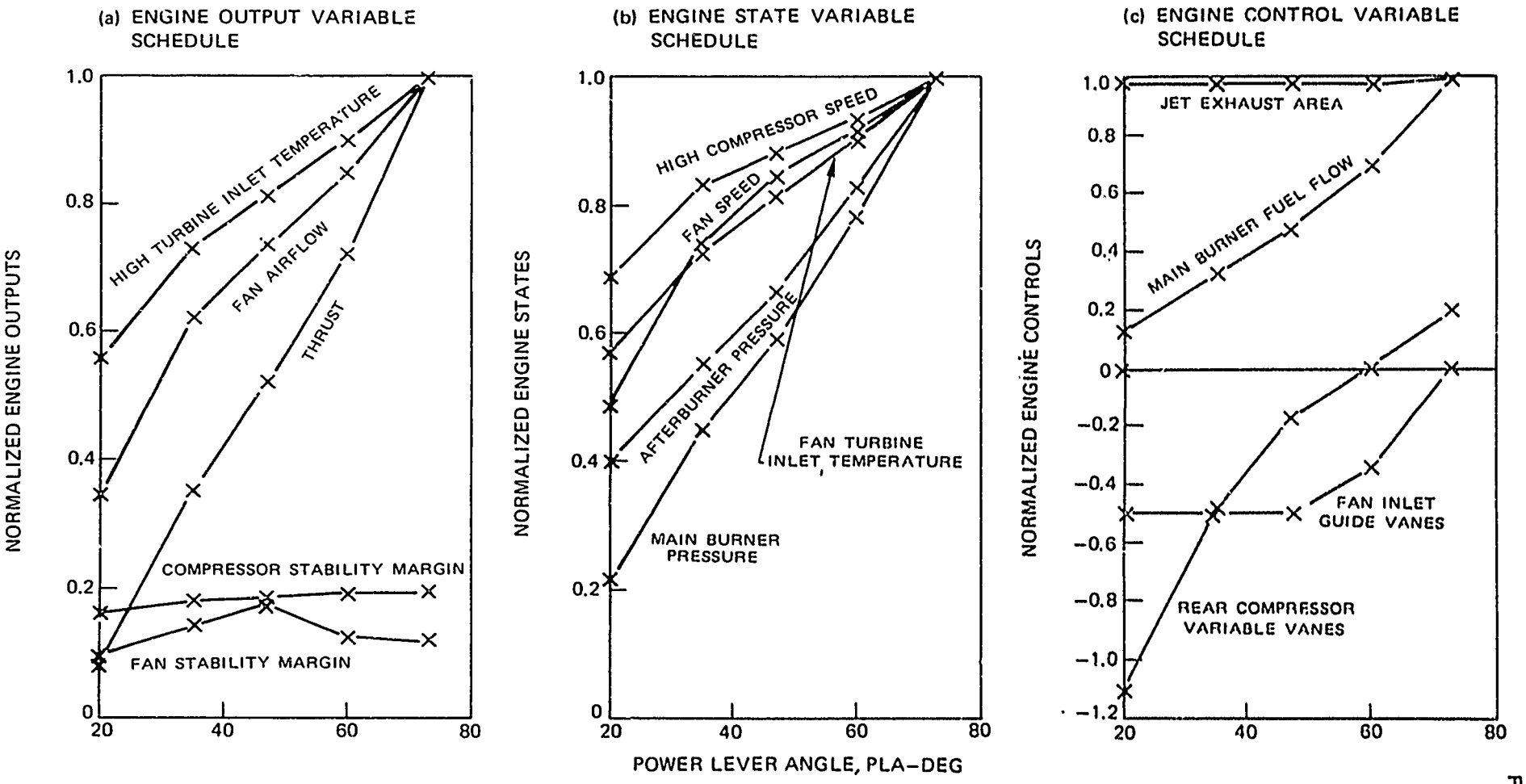

FIG. 1

N911620-2

FIG. 2

OPTIMAL CLOSED-LOOP STRUCTURES FOR STANDARD LINEAR AND INTEGRAL CONTROLS

(a) LINEAR PLANT AND CONTROL DYNAMICS AUGMENTED WITH INTEGRATORS

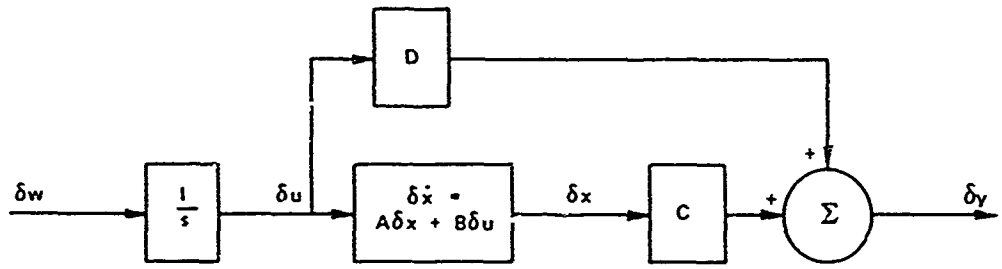

(b) STANDARD LINEAR OPTIMAL CONTROL

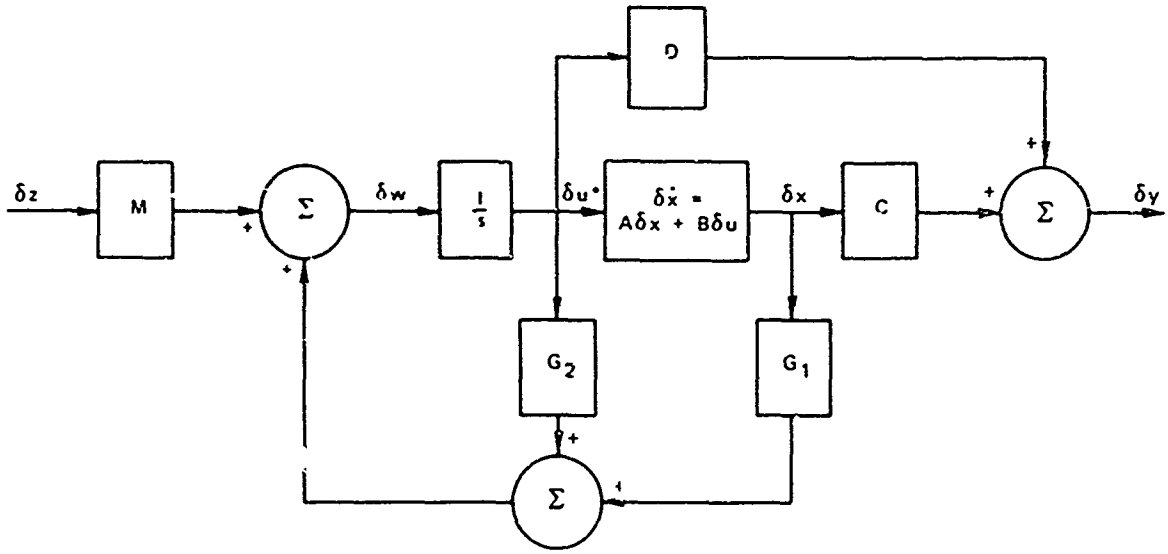

(c) OPTIMAL INTEGRAL CONTROL

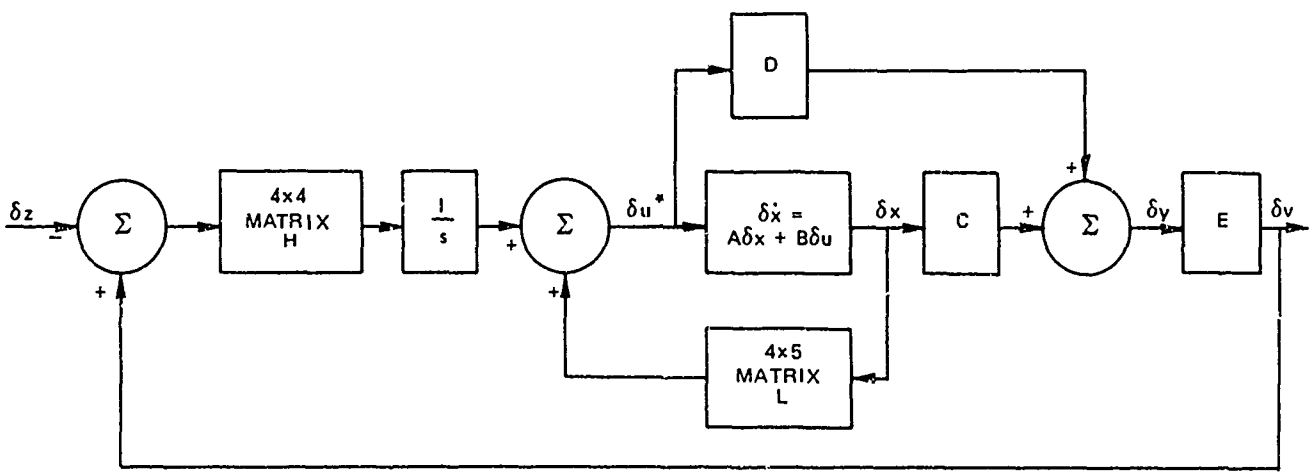

FIG. 3

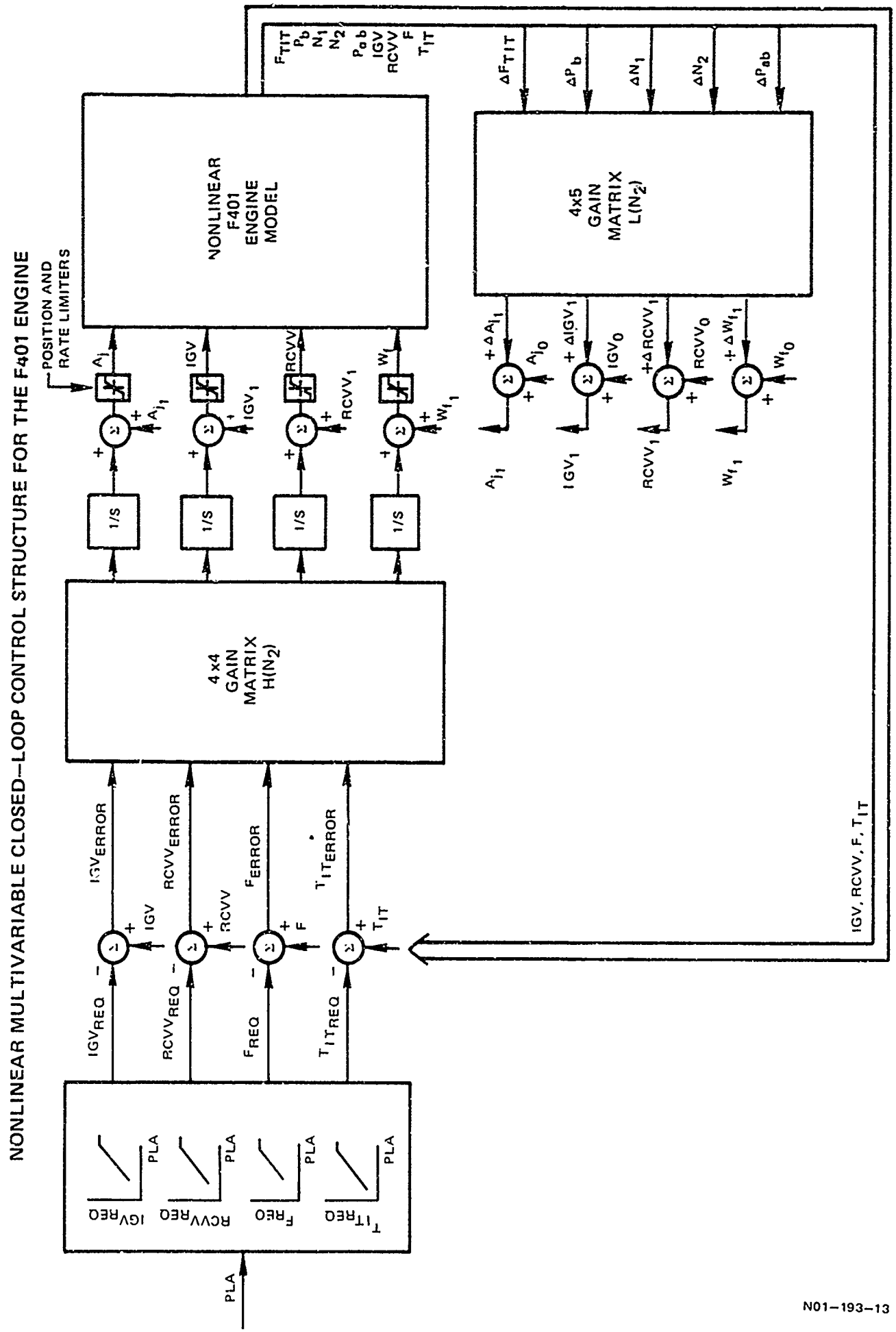
NONLINEAR MULTIVARIABLE CLOSED–LOOP CONTROL STRUCTURE FOR THE F401 ENGINE
NONLINEAR F401 ENGINE MODEL
POSITION AND RATE LIMITERS
4x4 GAIN MATRIX H(N2)
4x5 GAIN MATRIX L(N2)
1/S
PLA
IGV, RCVV, F, TIT
N01–193–13

N911620–2

NORMALIZED F401 THRUST RESPONSE FOR OPTIMAL AND CONVENTIONAL CONTROLLERS

THRUST RESPONSE PRODUCED BY STEP CHANGE IN PLA FROM 20 DEG (IDLE–9 PERCENT) TO 73 DEG (MILITARY–100 PERCENT)

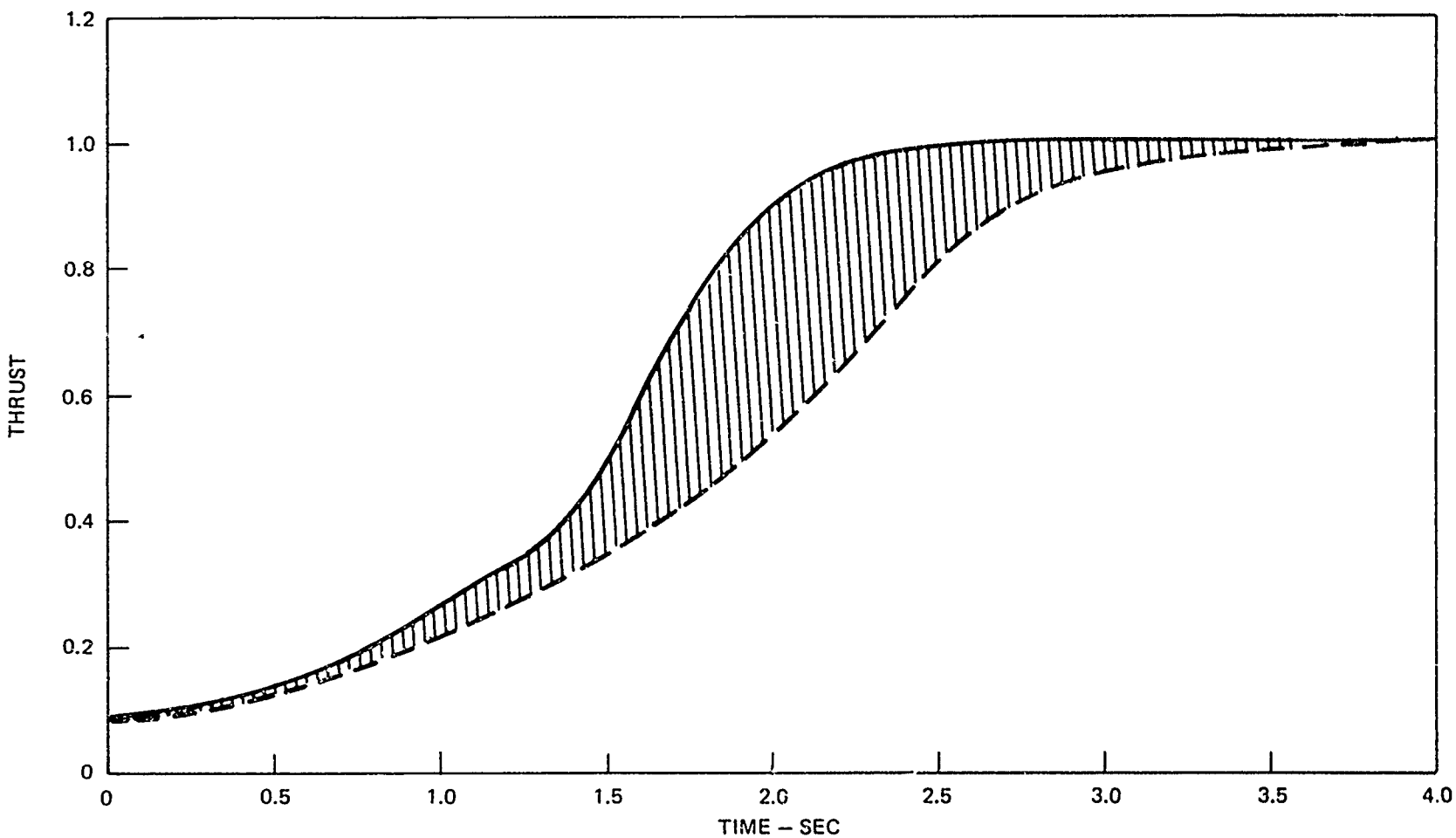

N02–89–3

FIG. 4

NORMALIZED F401 TEMPERATURE AND STABILITY MARGIN RESPONSES FOR OPTIMAL AND CONVENTIONAL CONTROLLERS

RESPONSES PRODUCED BY STEP CHANGE IN PLA FROM 20 DEG (IDLE–9 PERCENT) TO 73 DEG (MILITARY–100 PERCENT)

OPTIMAL MULTIVARIABLE CONTROLLER — CONVENTIONAL CONTROLLER

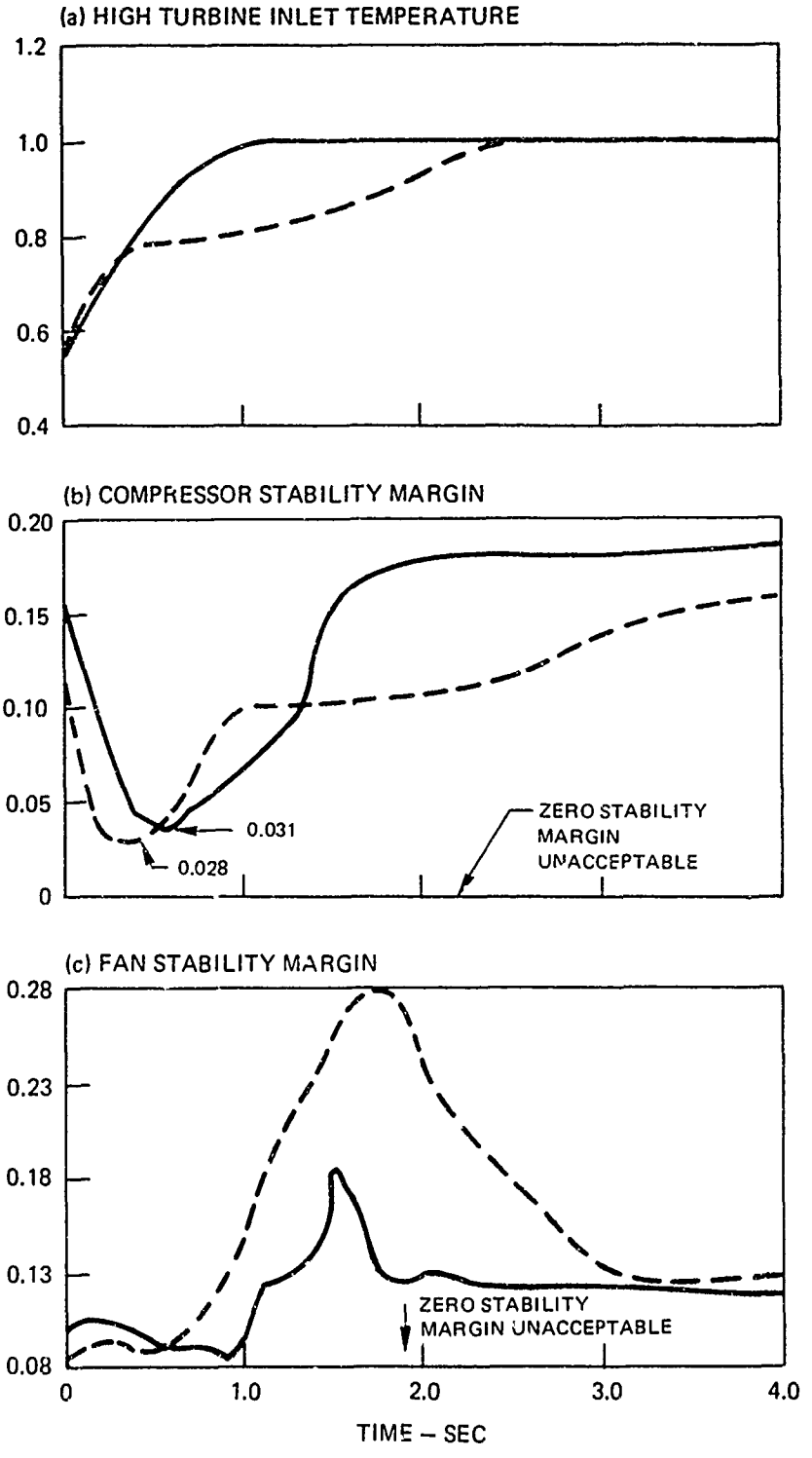

N02–89–4

NORMALIZED F401 SPOOL SPEED AND AIRFLOW RESPONSES FOR OPTIMAL AND CONVENTIONAL CONTROLLERS

RESPONSES PRODUCED BY STEP CHANGE IN PLA FROM 20 DEG (IDLE–9 PERCENT) TO 73 DEG (MILITARY–100 PERCENT)

——— OPTIMAL MULTIVARIABLE CONTROLLER – – – – CONVENTIONAL CONTROLLER

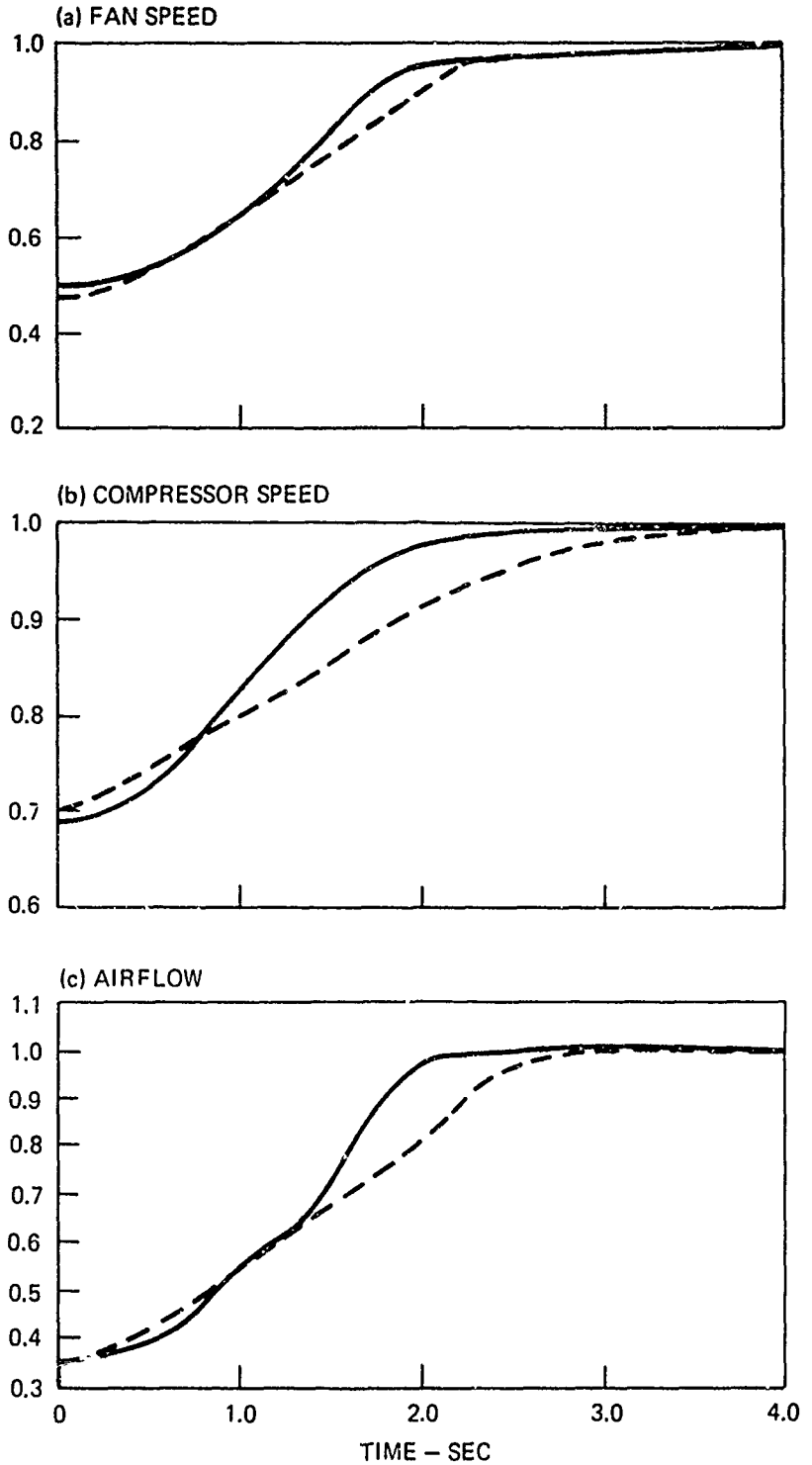

N02–89–5

FIG. 7

NORMALIZED F401 EXHAUST AREA RESPONSE FOR OPTIMAL AND CONVENTIONAL CONTROLLERS

EXHAUST AREA RESPONSE PRODUCED BY STEP CHANGE IN PLA FROM 20 DEG (IDLE–9 PERCENT) TO 73 DEG (MILITARY–100 PERCENT)

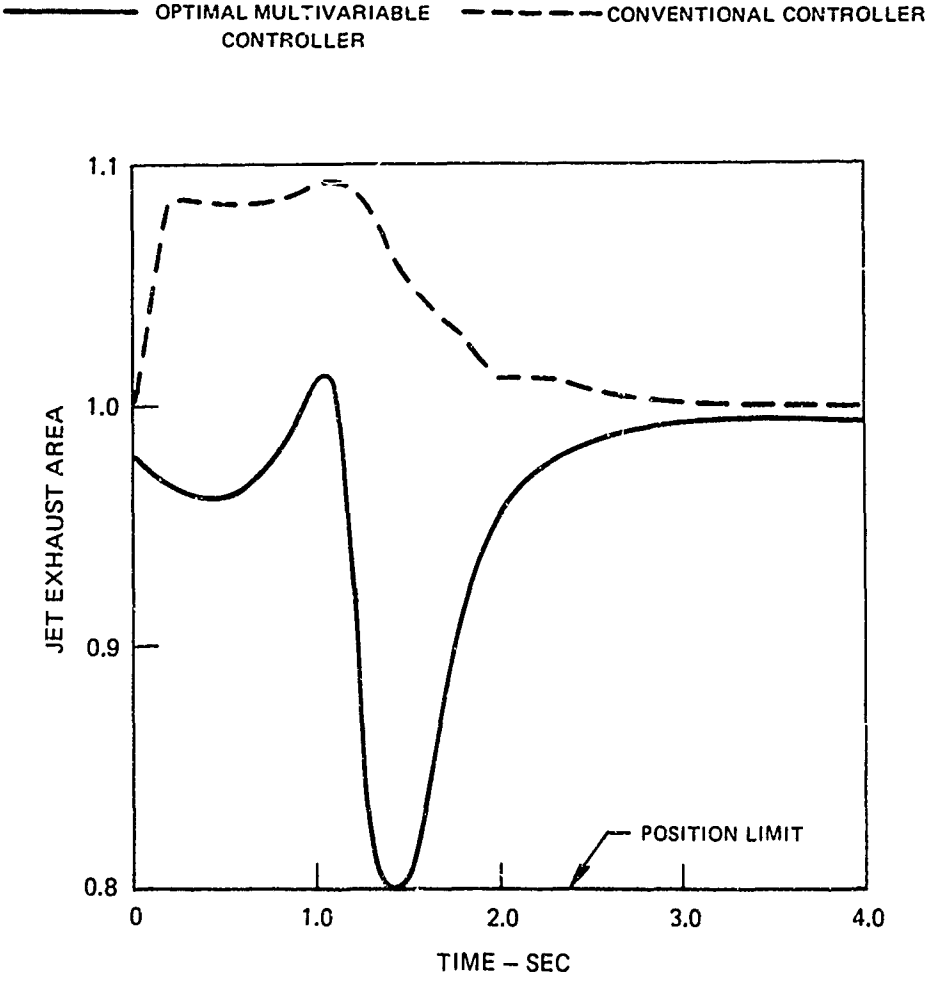

NORMALIZED F401 MAIN BURNER FUEL FLOW RESPONSE FOR OPTIMAL AND CONVENTIONAL CONTROLLERS

FUEL FLOW RESPONSE PRODUCED BY STEP CHANGE IN PLA FROM 20 DEG (IDLE–9 PERCENT) TO 73 DEG (MILITARY–100 PERCENT)

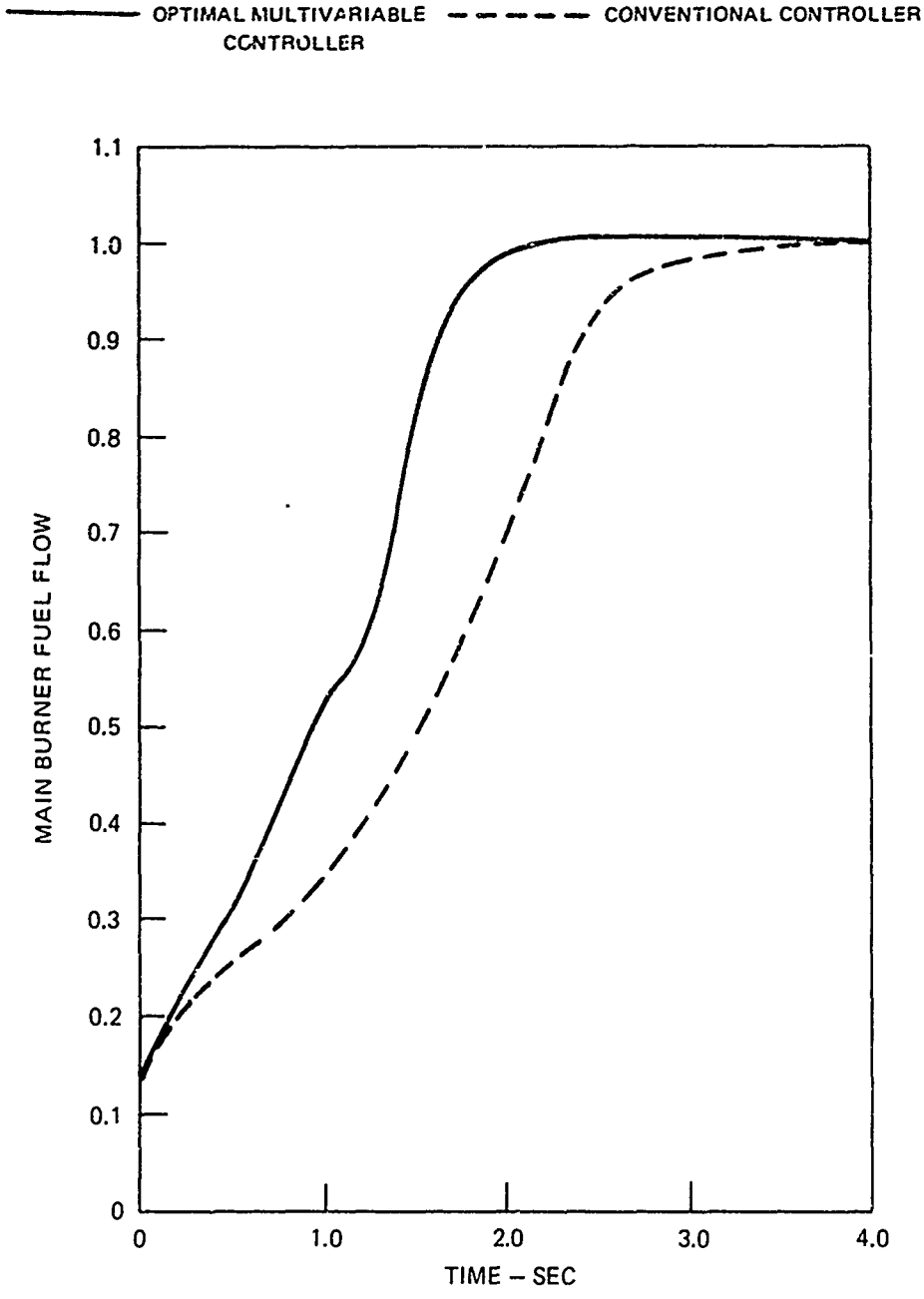

NORMALIZED F401 FAN INLET GUIDE VANE RESPONSE FOR OPTIMAL AND CONVENTIONAL CONTROLLERS

FAN INLET GUIDE VANE RESPONSE PRODUCED BY STEP CHANGE IN PLA FROM 20 DEG (IDLE–9 PERCENT) TO 73 DEG (MILITARY–100 PERCENT)

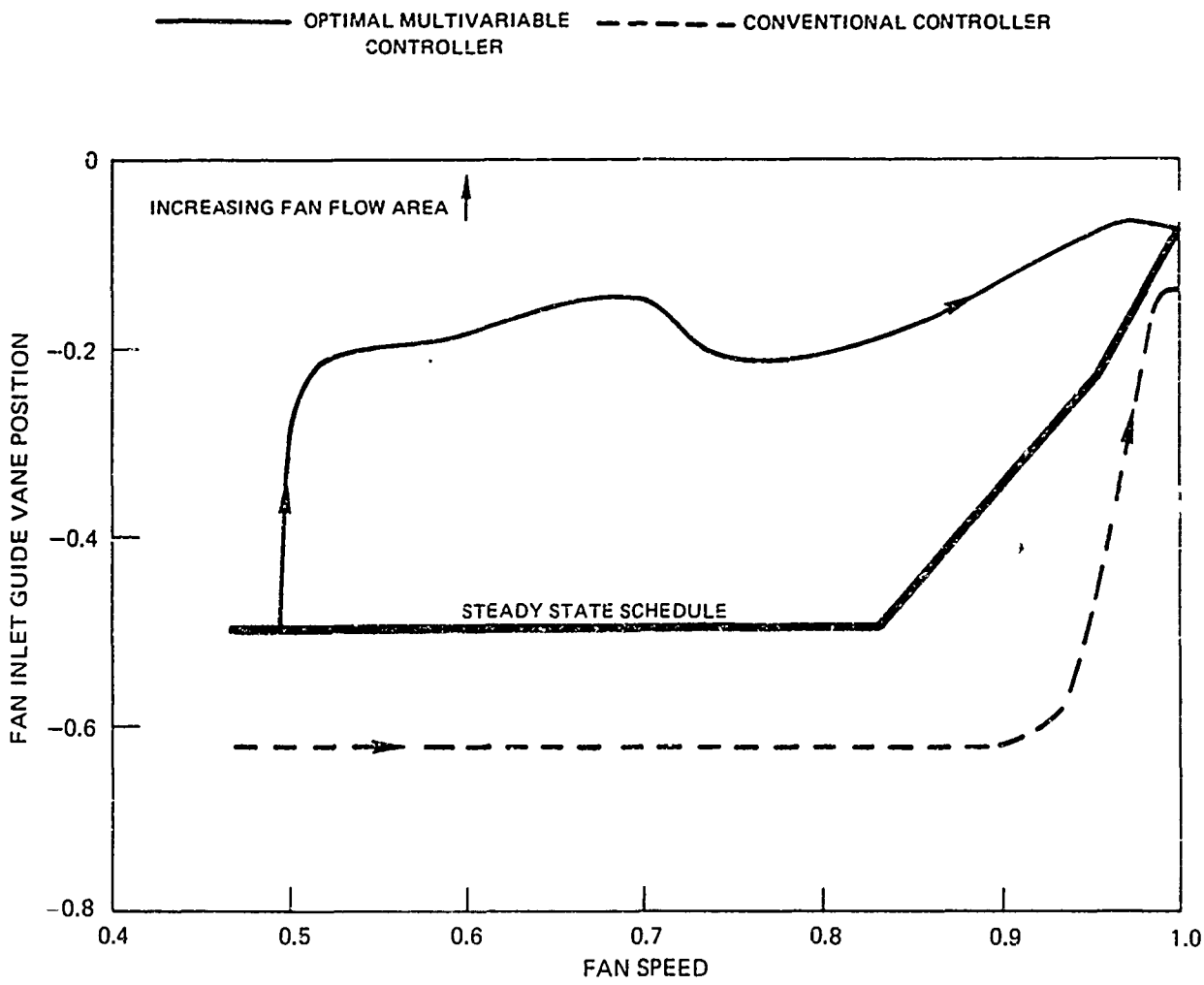

NORMALIZED F401 REAR COMPRESSOR VARIABLE VANE RESPONSE FOR OPTIMAL AND CONVENTIONAL CONTROLLERS

REAR COMPRESSOR VARIABLE VANE RESPONSE PRODUCED BY STEP CHANGE IN PLA FROM 20 DEG (IL -9 PERCENT) TO 73 DEG (MILITARY–100 PERCENT)

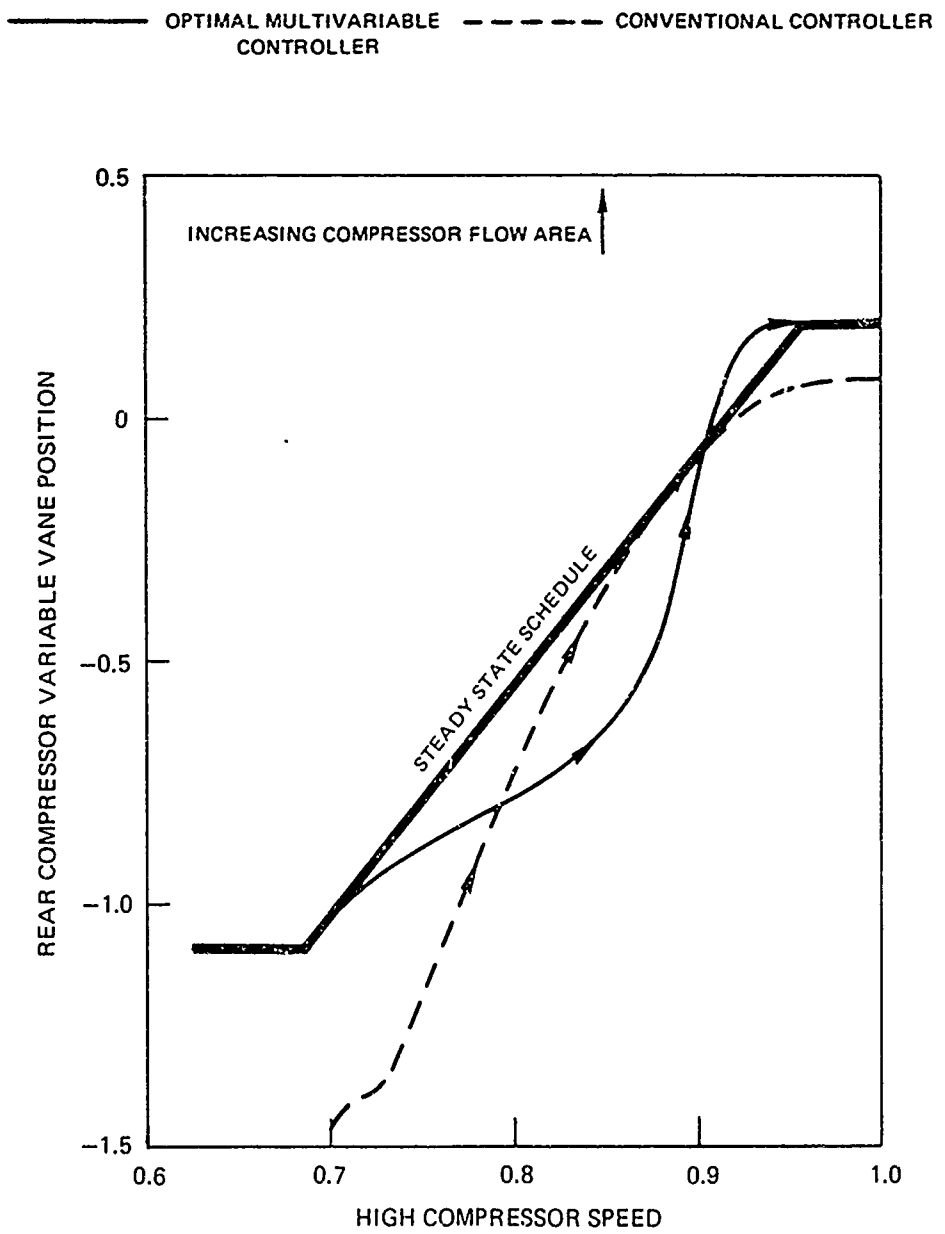

N02–89–6

N91620-2

LINEARIZED INTERNAL COMPRESSION SUPERSONIC INLET MODEL

PARAMETERS SHOWN FOR 40,000 FT, MACH 2.2 OPERATING POINT

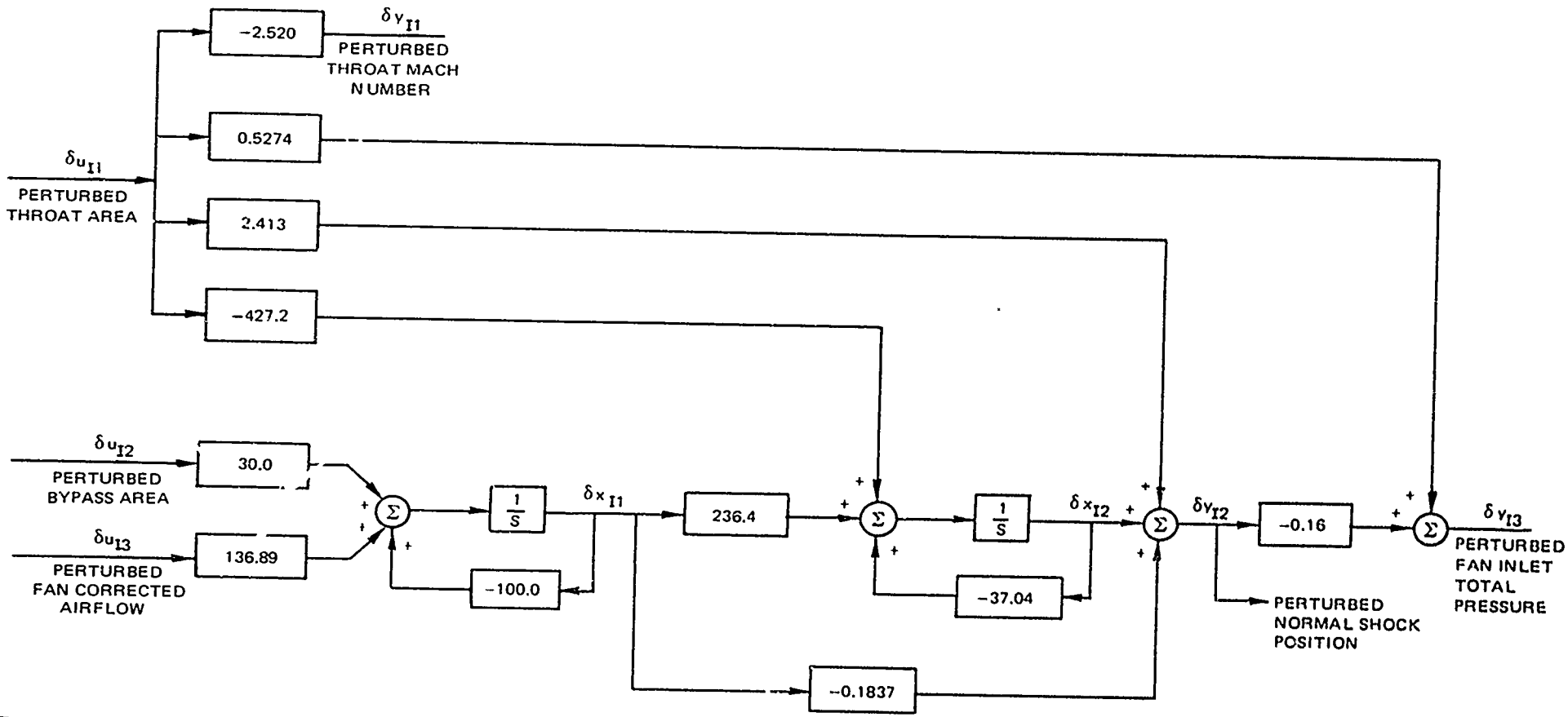

N02-89-12

FIG. 11

NORMALIZED INLET–ENGINE RESPONSE FOR INTEGRATED AND SEPARATE MULTIVARIABLE CONTROLLERS

PERTURBATIONS ABOUT NORMALIZED STEADY-STATE VALUES PRODUCED BY SIMULATED AFTERBURNER IGNITION

——— RESPONSE FOR INTEGRATED CONTROLLER

– – – – – RESPONSE FOR SEPARATE CONTROLLER

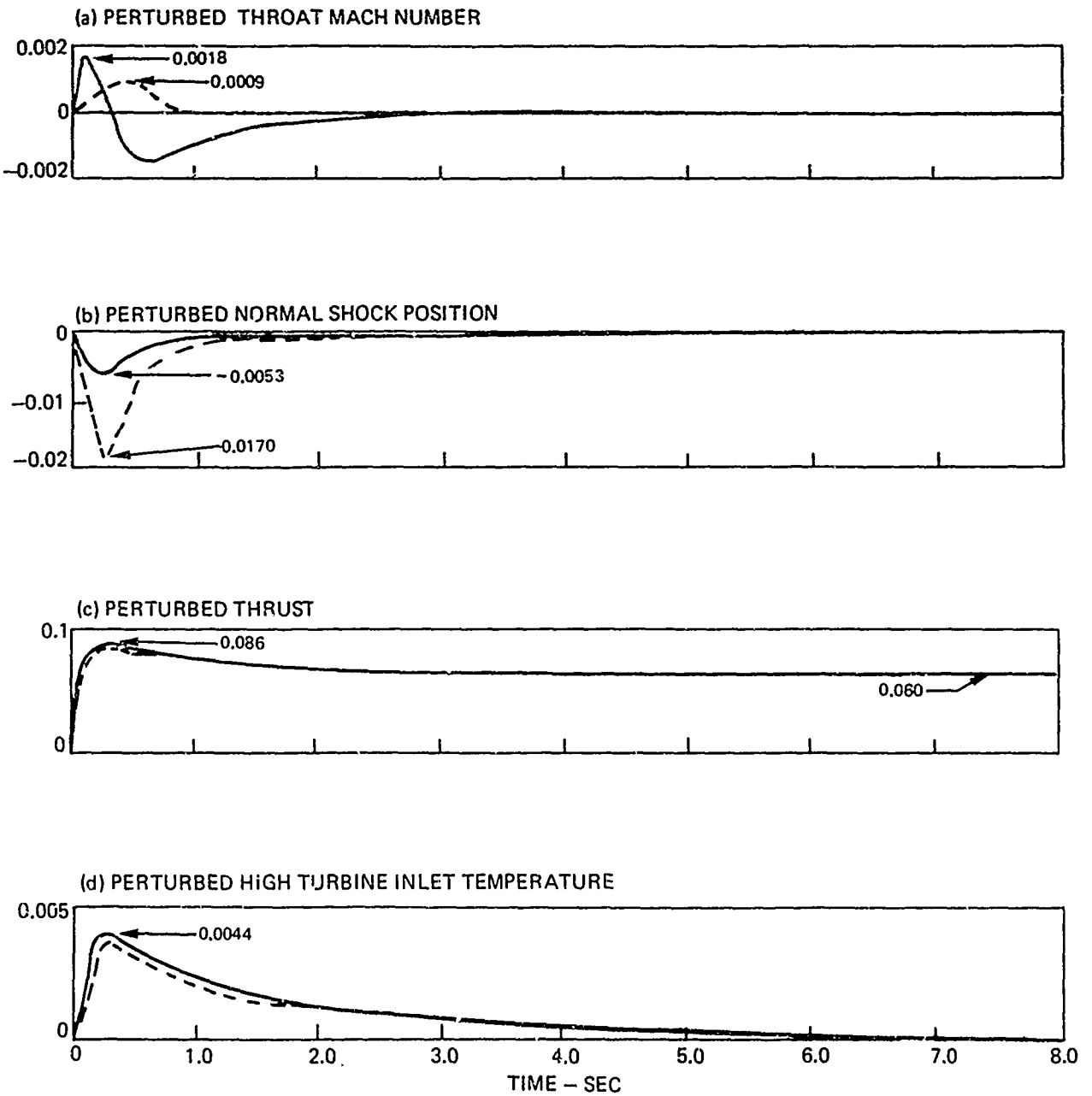

N02–89–11

CONT'D

NORMALIZED INLET–ENGINE RESPONSE FOR INTEGRATED AND SEPARATE MULTIVARIABLE CONTROLLERS

PERTURBATIONS ABOUT NORMALIZED STEADY-STATE VALUES
PRODUCED BY SIMULATED AFTERBURNER IGNITION

——— RESPONSE FOR INTEGRATED CONTROLLER

– – – – – RESPONSE FOR SEPARATE CONTROLLER

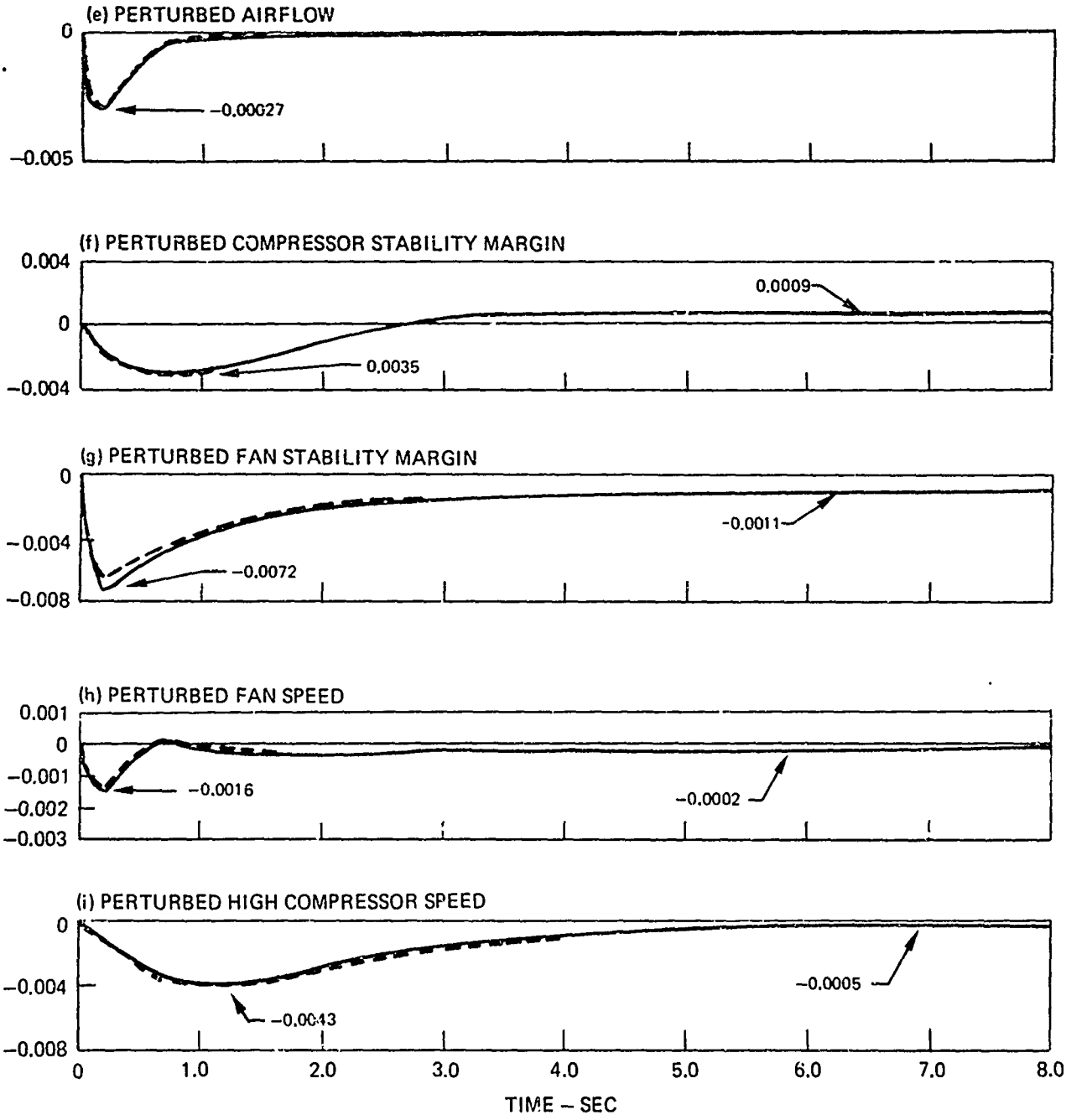

N02–89–13

NORMALIZED INLET–ENGINE RESPONSE FOR INTEGRATED AND SEPARATE MULTIVARIABLE CONTROLLERS

PERTURBATIONS ABOUT NORMALIZED STEADY-STATE VALUES
PRODUCED BY SIMULATED AFTERBURNER IGNITION

——— RESPONSE FOR INTEGRATED CONTROLLER

– – – – RESPONSE FOR SEPARATE CONTROLLER

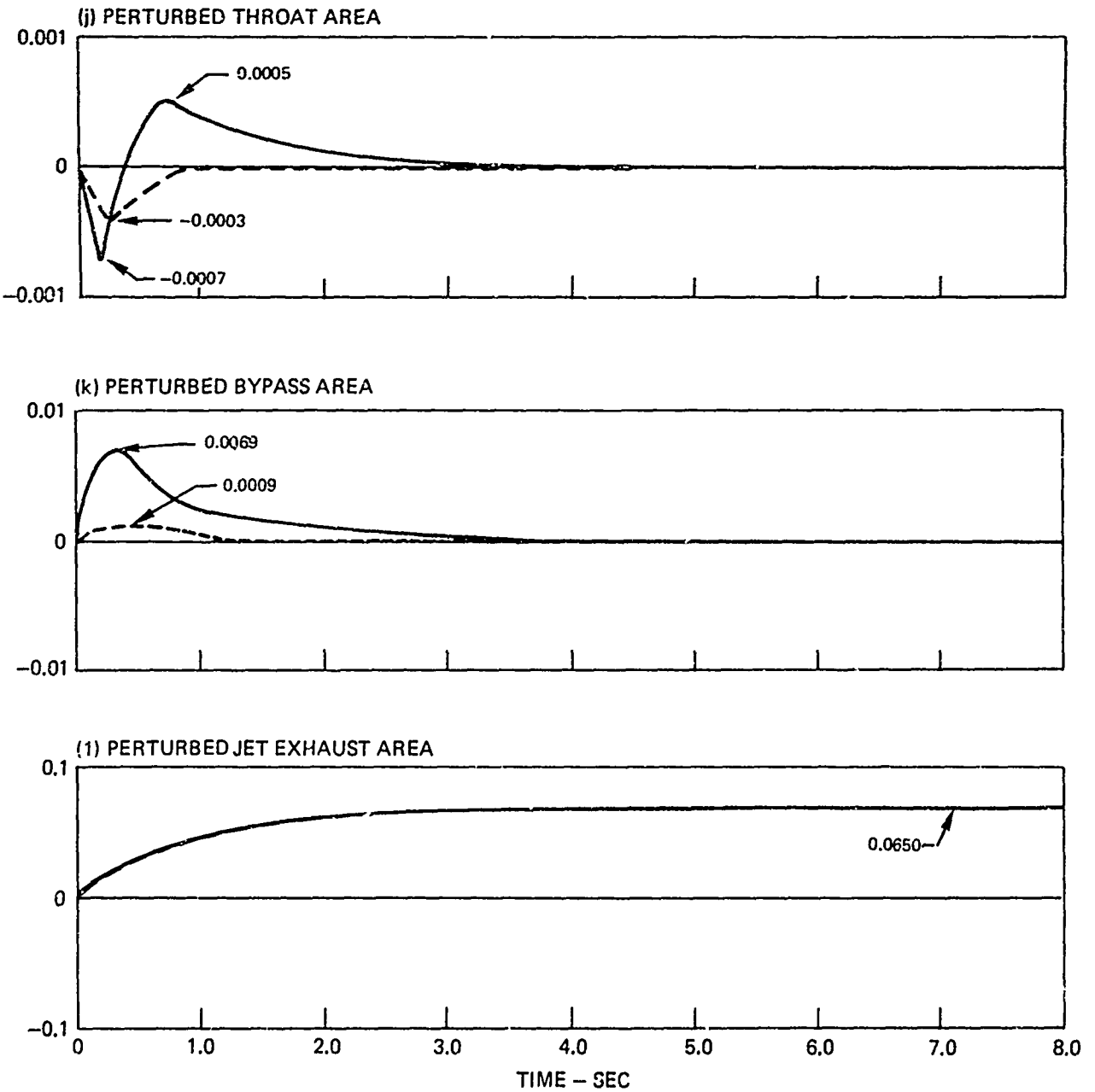

N02–89–8

CONT'D

FIG. 12(m)–(o)

NORMALIZED INLET–ENGINE RESPONSE FOR INTEGRATED AND SEPARATE MULTIVARIABLE CONTROLLERS

PERTURBATIONS ABOUT NORMALIZED STEADY-STATE VALUES
PRODUCED BY SIMULATED AFTERBURNER IGNITION

——— RESPONSE FOR INTEGRATED CONTROLLER

– – – – – RESPONSE FOR SEPARATE CONTROLLER

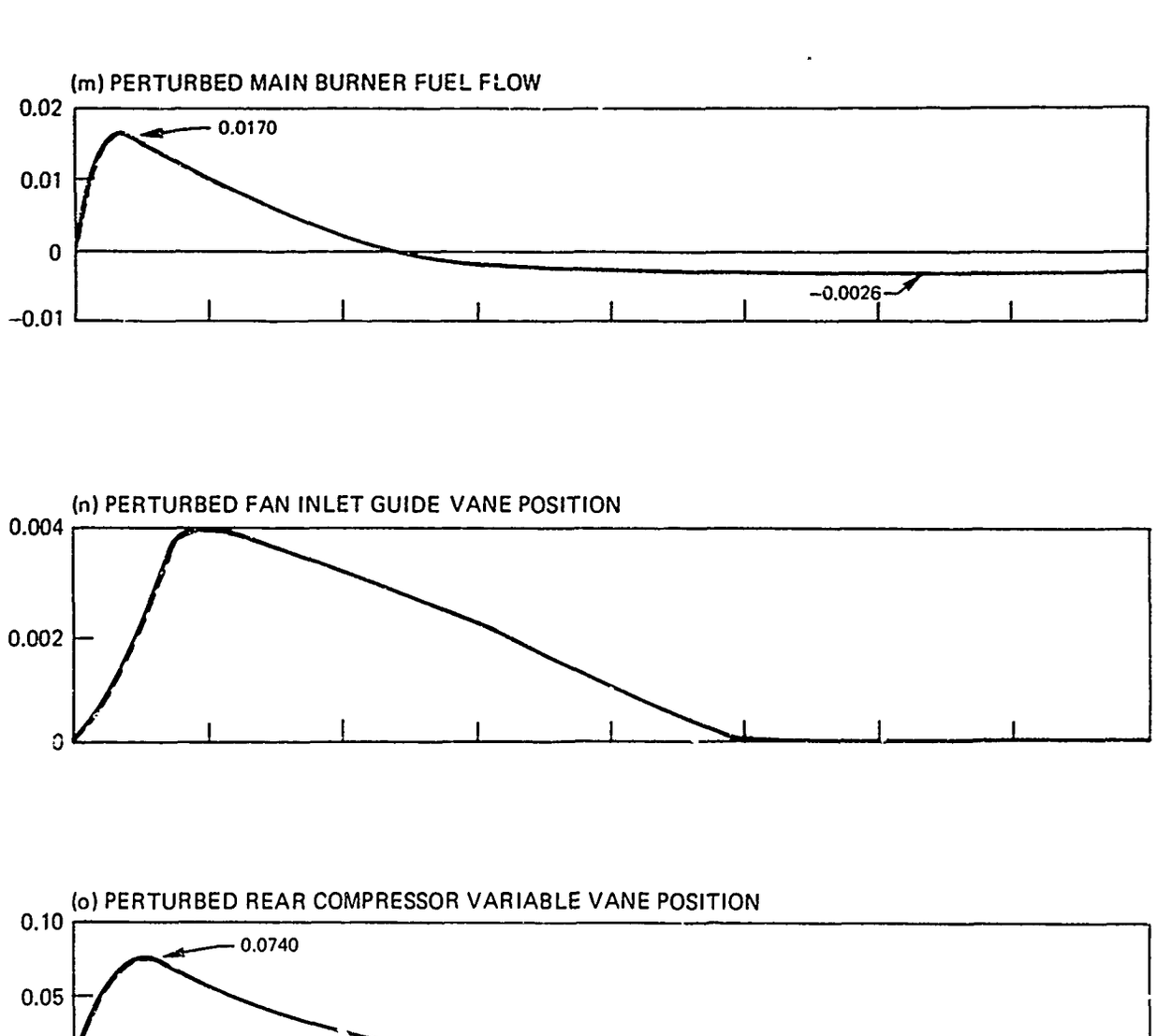

N02–89–7

NORMALIZED INLET–ENGINE RESPONSE FOR INTEGRATED AND SEPARATE CONTROLLERS WITH INCREASED WEIGHTING OF SHOCK POSITION IN INLET PERFORMANCE INDEX

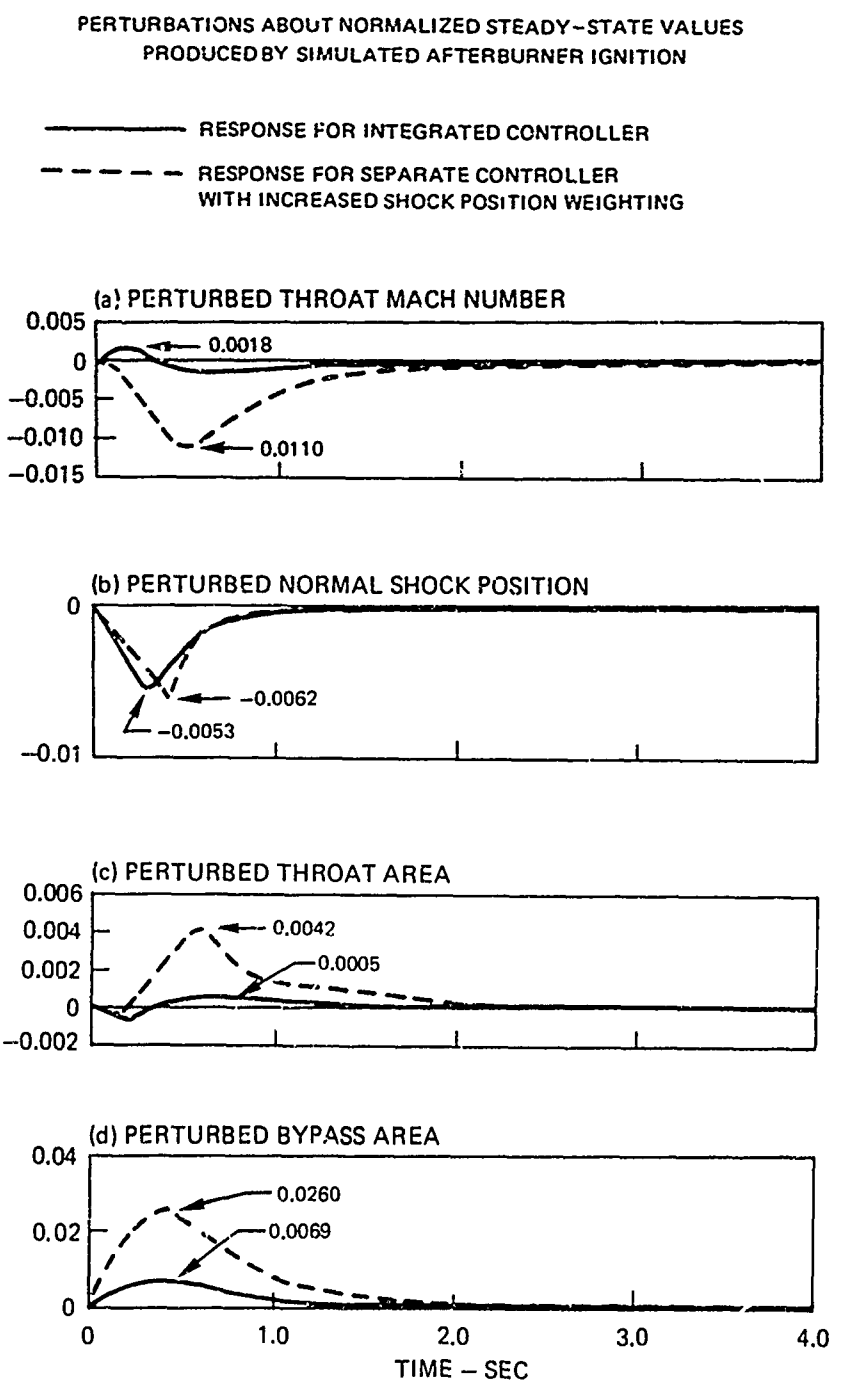

N02–89–9